Aalto University
School of Chemical
Technology

Tamer Alhalabi

CONTAMINANTS REMOVAL BY HOT VAPOUR FILTRATION

Master´s Programme in Chemical, Biochemical and Materials Engineering

Major in Biomass Refining

Master's thesis for the degree of Master of Science in Technology submitted for inspection, Espoo, 2 September, 2019.

Supervisor	Professor Ville Alopaeus
Instructor	M.Sc. Christian Lindfors

Aalto University
School of Chemical
Engineering

Aalto University, P.O. BOX 11000, 00076 AALTO
www.aalto.fi

Abstract of master's thesis

Author Tamer Alhalabi

Title of thesis CONTAMINANTS REMOVAL BY HOT VAPOUR FILTRATION

Degree Programme Chemical, Biochemical and Materials Engineering

Major Biomass refining

Thesis supervisor Professor Ville Alopaeus

Thesis advisor(s) / Thesis examiner(s) M.Sc. (Tech.) Christian Lindfors

Date 02.09.2019 **Number of pages** 76 **Language** English

Abstract: Ongoing interest in producing high quality fast pyrolysis oil is the drive behind this subject. This thesis is set to investigate the separation of solids contaminants by incorporating a hot vapour filter in a bench-scale (1kg/h) fast pyrolysis setup. The hot filter consists of ceramic candles and moving granules for filtration and cake regeneration purposes, respectively. Qualitative and quantitative analysis of pyrolytic products have been carried out; to investigate the influence of different filtration temperatures. Furthermore, upscaling and integration of the hot filter with an existing pilot-scale plant have been studied.

Recycled wood containing solid contaminants, alkali and alkaline earth metals (AAEM) was pyrolysed in a bubbling fluidised-bed reactor. The optimum pyrolysis temperature for recycled wood was 500 °C, which resulted in a maximum organic yield of 55 wt. % on dry basis. Incorporating the hot filter led to significant reduction in organic yield. Among the tested filtration temperatures, 360 °C was the optimal temperature yielding 48 wt. % of organics on dry basis. Filtered bio-oil exhibited lower alkali and alkaline earth metals than unfiltered bio-oil. Furthermore, filtered bio-oils demonstrated better stability during storage. However, despite the low solids content and the reduction of AAEM, ageing reactions continued to develop during storage, but at a lower rate than unfiltered bio-oil.

Constant differential pressure across the hot filter was maintained during 6 h run at 360 °C; implying an efficient regeneration of char cake over filtration candles. Moving granules break down the accumulated chars over the ceramic surface, and act as filtration media for particle-laden vapours. Upscaling of hot filter and its integration with a circulating fluidised-bed is considered at the end of the study. Preliminary design of pilot filter is based on a calculated face velocity of 2.03 cm/s. Such a scalability study is necessary to evaluate the viability of the technology at a large scale.

Keywords Hot vapour filtration, alkali earth metals, upgrading technology, granules, ceramic candles, fast pyrolysis, bio-oil.

Acknowledgements

Presented thesis was written at VTT Technical Research Centre of Finland Ltd during spring and summer of 2019. I would like to thank everyone who made this possible. Special thanks to my advisor Christian Lindfors for his guidance and to my supervisor Ville Alopaeus for his contribution towards the subject. Special gratitude goes to Elmeri Pienihäkkinen and Joona Lahtinen, who helped me during experimentations. I would like to also thank Elina Raineva, Jaana Korhonen and Sirpa Lehtinen for their professional work in the laboratory. Last but not least, huge thanks to my family for their unwavering support.

Table of contents

List of abbreviations

Acronyms

AAEMs	Alkali and alkaline earth metals
ASTM	American society for testing and materials
BTG	Biomass Technology Group
BFB	Bubbling Fluidised-Bed
CEN	European Committee for Standardization
CFB	Circulating Fluidised Bed
CHP	Combined Heat and Power
ES	Ether Soluble
FPBO	Fast Pyrolysis Bio-Oil
HDO	Hydrodeoxygenation
HTU	Hydrothermal Upgrading
HVF	Hot Vapour Filtration
HWE	Hot Water Extraction
HZSM-5	Acidic Zeolite Socony-Mobil 5
IGCC	Integrated Gasification and Combined Cycle
p-TSA	P-toluenesulfonic Acid
MGBF	Moving Granular Bed Filter
NCG	Non-Condensable gases
NREL	National Renewable Energy Laboratory
PFBC	Pressurized Fluidised Bed Combustion
PNNL	Pacific Northwest National Laboratory
SE	Steam Explosion
TAN	Total Acid Number
VTT	Technical Research Centre of Finland
WS	Water Soluble
WIS	Water Insoluble
ZSM-5	Zeolite Socony-Mobil 5

List of figures

List of tables

Literature Review

1. Introduction

1.1 Background

Energy demand is on the rise, and institutional reliance on fossil fuels has a self-perpetuating inertia. However, as renewable technologies advance, more cost effective remedies arise. Several biomass utilization technologies have evolved in the past decade. Biomass can be deployed in different thermal conversion technologies. The most common thermal conversion processes are pyrolysis, gasification, combustion and hydrothermal processing. Among these technologies, pyrolysis emerges as a promising process to diversify the energy resources. Unlike the other thermal conversion technologies, pyrolysis favors production of hydrocarbon liquids. Fast pyrolysis bio-oils (FPBO) can be valorized into different biofuel grades which have the potential to replace the dominating fossil-based fuels. Compared to gasification, combustion and hydrothermal processing products, pyrolysis liquids are highly dense with 2.5-3.5 times the energy density of softwood. In addition to that, pyrolysis liquids are easier to handle compared to gases and raw materials. Furthermore, pyrolysis liquids are more flexible; they can be utilized in power production as light or heavy fuels (Oasmaa et al. 2005).

Pyrolysis process decomposes the exploited biomass in inert conditions at elevated temperatures. Depending on the biomass residence time, the process is categorized as slow and fast pyrolysis. Slow pyrolysis process requires few hours to complete and favors production of bio-char as the main product. Whereas, fast pyrolysis reaction time is only in seconds and produces bio-oil alongside bio-char and gaseous phase. FPBO is produced at temperatures, between 450 and 600 °C. (Kan et al. 2016)

Compared to conventional fossil-based oil, fast pyrolysis bio-oil (FPBO) is chemically and thermally less stable. The instability is caused by the presence of reactive oxygen-rich compounds, e.g. aldehydes and ketones. These compounds promote the ageing reactions of bio-oil. Bio-oil ageing reactions impose storage and upgrading challenges (Lehto et al. 2013). Generally, bio-oil contains less than 0.5 wt. % of solids content. The presence of inorganic solids such as elutriated sand and metals contribute further to the ageing effect, and worsen storage conditions by creating sludge

layers, which lead to fouling in process equipment and limit utilization of bio-oil as a refinery feedstock and as a fuel (Lehto et al. 2013).

Several solid removal techniques have been investigated. Methods like pretreatment of feedstock prior to fast pyrolysis process, filtration of liquid bio-oil and filtration of pyrolytic vapours. This thesis will focus on the promising hot vapour filtration technique of solid particles removal from FPBO.

1.2 Structure

Starting with literature review in chapter 2 regarding fast pyrolysis process. The main principle of the process will be presented, in addition to the most commonly used reactor designs. Physio-chemical properties of FPBO will be introduced in the same chapter to highlight bio-oil limitations as a comparison with the conventional mineral oil. Chapter will end with an innovative successful integration story of the process at a commercial scale.

Chapter 3 will provide an overview of the promising FPBO upgrading technologies. The upgrading methods were categorized as chemical methods; such as hydrodeoxygenation, zeolite cracking, hydrothermal treatment and esterification. In addition to physical upgrading methods; such as pretreatment of biomass, liquid filtration and hot vapour filtration.

In depth review about hot vapour filtration technology will be presented in chapter 4. Starting with its principle, and the commonly used filter designs with their different filtration media. The literature review is wrapped with several research and development activities regarding the process. The section covers different experiments and innovative developments done by National Renewable Energy Laboratory (NREL), Pacific Northwest National Laboratory (PNNL), University of Twente, Technical Research Centre of Finland (VTT), Mahasarakham University, Aston University and Shanghai Jiao Tong University.

1.3 Objectives

Objective of this thesis is to highlight the technical feasibility of hot vapour filtration technology, with practical experiments that emphasize its performance as a contaminants removal technique. The filtration unit will be integrated into a bench-scale fast pyrolysis setup. Bio-oil yield and quality will be analyzed to study the viability of such an integration, and the effect of contaminants removal. The generated data from these experiments will be used for studying the practicalities of upscaling the filtration unit.

2. Fast pyrolysis

2.1 Principle

Fast pyrolysis is fundamentally defined as quick thermal decomposition of biomass in the absence of oxygen prior to rapid quenching of produced vapours. Depending on the utilized feedstock, a typical fast pyrolysis process yields 60-75 wt. % (dry-feed basis) of liquid bio-oil, alongside 15-25 wt. % of solid char, as well as 10-20 wt. % of non-condensable gases (Balat et al. 2009). Short vapour residence time, effective heat transfer, cautious control of temperature and rapid quenching of pyrolytic vapours are the main features of a fast pyrolysis process (Balat et al. 2009).

Liquid bio-oil is the main targeted product produced by fast pyrolysis. A typical process applies high heating rates (> 10^3 °C/s) and short residence times (0.5-10 seconds); residence time of less than 2 seconds is mostly implemented (Demirbas et al. 2002). In fast pyrolysis, low temperatures and longer residence time favor the production of bio-char. High temperatures and longer residence time conditions produce more products in gaseous phase. Whereas, moderate temperatures and shorter residence time process yields more bio-oil (Bridgwater, 2012).

A typical fast pyrolysis system comprises feedstock pretreatment stages of drying and grinding; where feedstock is dried to achieve a moisture content of 10-15 wt. %, and grinded to the required particle size to attain high heating rates (Bridgwater and Peacocke, 2000). Separating solids prior to the quenching stage of liquid oil is vital; to minimize the quantity of char and bed materials accumulation in the final product. Therefore, cyclones are often employed and placed after the reactor as a conventional method for solids separation.

Pyrolysis gaseous products consist of aerosols, condensable and non-condensable gases. In standard fast pyrolysis configurations, electro-static precipitation is considered an effective method for removing aerosols. Aerosols are partially depolymerized lignin particles with high molecular weight. Collection of aerosols is important since they are liquid basis contaminants originated from incomplete reactions (Bridgwater, 2012).

Since fast pyrolysis is an endothermic process, it requires considerable heating to reach reaction temperature. Commercial reactors designs are constantly optimized to achieve sufficient heat transfer. Energy stored in fast pyrolysis by-products such as in char or gas can be utilized to optimize a commercial unit. Bio-char contains 25% of feedstock energy which can cover 75% of the energy required to run the process. Combusting pyrolysis gas alone is insufficient, since it holds only 5% of feedstock energy (Bridgwater, 2012).

2.2 Fast pyrolysis reactors

Variety of reactor designs are implemented to achieve optimum decomposition of biomass in the absence of oxygen. Reactors such as rotating cone, ablative reactor, bubbling and circulating fluidised bed are consistently optimized to accomplish two essential conditions for liquid production: an ideal heat transfer and very low vapours residence time. Rapid heat transfer assures quick heating of feedstock particles at low temperatures. Whereas, low vapours residence time diminishes secondary reactions (San Miguel et al. 2012).

Table 1 shows a summary of reactors characteristics regarding feed size requirement, carrier gas requirement, bio-oil yields, complexity, scalability and their current status (Kan et al. 2016). Required feed moisture for all these reactors is less than 10 % (Kan et al. 2016). Condensable products in fluidised beds have lower partial pressure than in rotating cone and ablative reactors, due to the high quantity of fluidizing carrier gas. Tightly-packed equipment and lower costs are associated with less usage of carrier gas (Bridgwater 2012). Various reactor designs demand different particle sizes. Feedstock particle size ranges between less than 0.2-6 mm for rotating cone reactors and whole tree chips for ablative reactors. Whereas, bubbling and circulating fluidised bed utilize particles size of less than 2mm and 6mm, respectively (Kan et al. 2016). Reactors with low attrition of chars reduce the formation of carbon fines-tainted vapours. Specific particles size

requirement for some reactors weighs heavily on feedstock preparation stage, making it an energy- and money-intensive process (San Miguel et al. 2012).

Table 1: Commercial scale pyrolysis reactors attributes (Modified table from Kan et al. 2016).

Reactor type	Feed size requirement	Carrier gas need	Bio-oil yield (wt. %)	Complexity	Scalability	Tested Scale	Status
Bubbling Fluidised bed	< 2 mm	High	75%	Medium	Easy	2-20 t/h	Commercial
Circulating Fluidised bed	< 6 mm	High	75%	High	Easy	2-20 t/h	Commercial
Rotating cone	< 0.2-6 mm	Low	70%	High	Medium	200-2000 kg/h	Commercial
Ablative	< 20 mm	Low	75%	High	Hard	1-20 kg/h	laboratory

2.2.1 Bubbling fluidised bed

Bubbling Fluidised bed (BFB) is a mature technology with uncomplicated reactor design. Feedstock particle size of less than 2mm is needed to achieve high heating rates. Heat transfer within the reactor is efficient as the bed holds sand with a particle size of about 250 μm (Venderbosch, 2010). Fluidised bed pyrolyser is relatively easy to operate with good temperature control. Bubbling fluidised bed scalability is very well understood despite heat transfer limitations at large scales (Bridgwater, 2012). The needed heat can be generated either by combusting the produced by-products (char and gas), or by heating coils. The latter heating option seems to have limited scalability (Venderbosch and Prins, 2010). Figure 1 shows an integrated bubbling fluidised-bed within a fast pyrolysis process. Char leaves the fluidised-bed by overflow alongside pyrolytic vapours. Cyclones are typically used to separate char. Cyclonic separation is a very well-studied technology, that is easy to scale up. Condensable vapours are rapidly quenched to get bio-oil. Whereas, aerosols are collected in an electrostatic precipitator before recycling part of the non-condensable gases for fluidisation purposes.

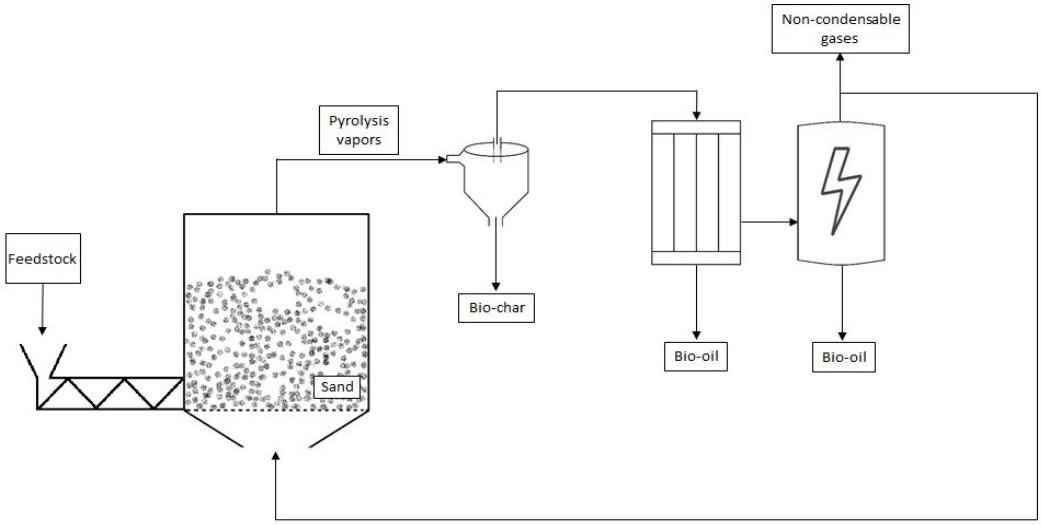

Figure 1: Bubbling Fluidised bed in a typical fast pyrolysis process

(Figure re-created based on Venderbosch, 2010, San Miguel et al. 2012 and Bridgwater 2012).

2.2.2 Circulating Fluidised bed

Circulation of biomass and sand through a cyclone and a combustor is the main principle behind circulating fluidised-beds (CFB). This technology was the outcome of a research done by the University of Ontario, started in late 1970s (Powell, 2010). Char and sand are separated from pyrolytic vapours by cyclones prior to the full recirculation of sand to the reactor through a char combustor, as shown in figure 2. The produced combustible char is an efficient source of energy for this technology. Heat transfer inside the reactor is 80% conduction, 19% convection and 1% radiation (Bridgwater, 1999). Pyrolytic vapours are rapidly quenched in multiple stages, and side stream of the non-condensable gases is circulated back to maintain an efficient circulation of materials through the reactor. The circulation technology commercialized the rapid thermal processing of biomass. Ensyn commercialized this technology at different capacities of 650 kg/h, 1700 kg/h and 2000 kg/h in Italy, USA and Canada, respectively (Bridgwater, 2012). Accurate temperature control and the ability to process substantial amounts of biomass with large particle sizes make this technology a commercially viable option. Utilization of large amounts of carrier gas dilutes pyrolytic vapours and makes bio-oil recovery a challenging task. In addition, high sand and char attrition; due to complex hydrodynamics and high velocities, leads to the production of char and sand-tainted bio-oil (Garcia-Nunes et al. 2017).

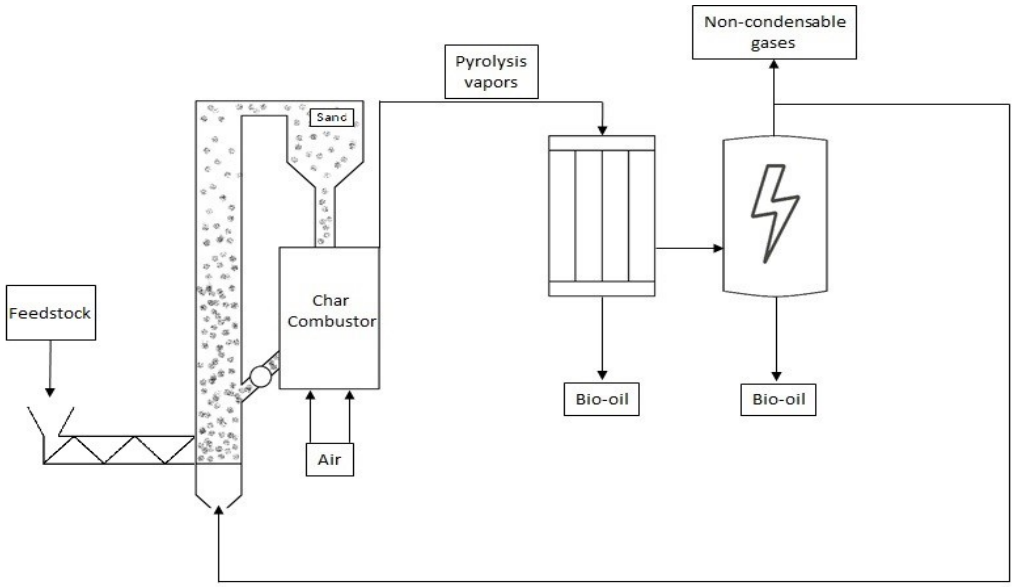

Figure 2: Circulating fluidised bed integrated in a typical fast pyrolysis process.
(Figure re-created based on Venderbosch, 2010, San Miguel et al. 2012 and Bridgwater 2012).

2.2.3 Rotating cone

Based on mixing hot sand with feedstock to achieve efficient decomposition of biomass, Twente University in the Netherlands developed rotating cone reactor. The reactor is designed to overcome the excess utilization of carrier gases needed for fluidisation. Instead, mechanical mixing of biomass and sand inside a rotating cone is fulfilled. Biomass and sand are placed at the bottom of the cone. Centrifugal forces transport biomass-sand mixture upward across the hot rotating cone; where pyrolysis reactions take place (Venderbosch and Prins, 2010). Intense mixing decomposes biomass into pyrolytic vapours which are rapidly quenched. Whereas, the produced char ultimately falls off the edge of the rotating cone alongside the sand. The falling char is combusted to heat the sand bubbling bed inside the combustor chamber, as shown in figure 3. Less amounts of carrier gas are employed in the riser to transport the heated sand upward for circulation. Integration of rotating cone designs, sand transporting riser and bubbling bed char combustor is considered challenging to achieve (Bahng et al. 2009). Biomass Technology Group (BTG) in the Netherlands scaled up the rotating cone reactor concept to process 260 kg/h. The revolving speed of the cone reactor is 300 rpm. It operates at 500 °C and yields 70 wt. %, 15 wt. % and 15 wt. % of bio-oil, char and non-condensable gases, respectively. Also in the Netherlands, Empyro consortium constructed a fast pyrolysis commercial demonstration plant based on rotating cone reactor concept. It has an

operational capacity of 120 tons per day. The produced bio-oil is utilized in heating applications (Perkins et al. 2018). Scalability of such a design is possible by stacking several cones on a single axis and by increasing the rotating cone diameter.

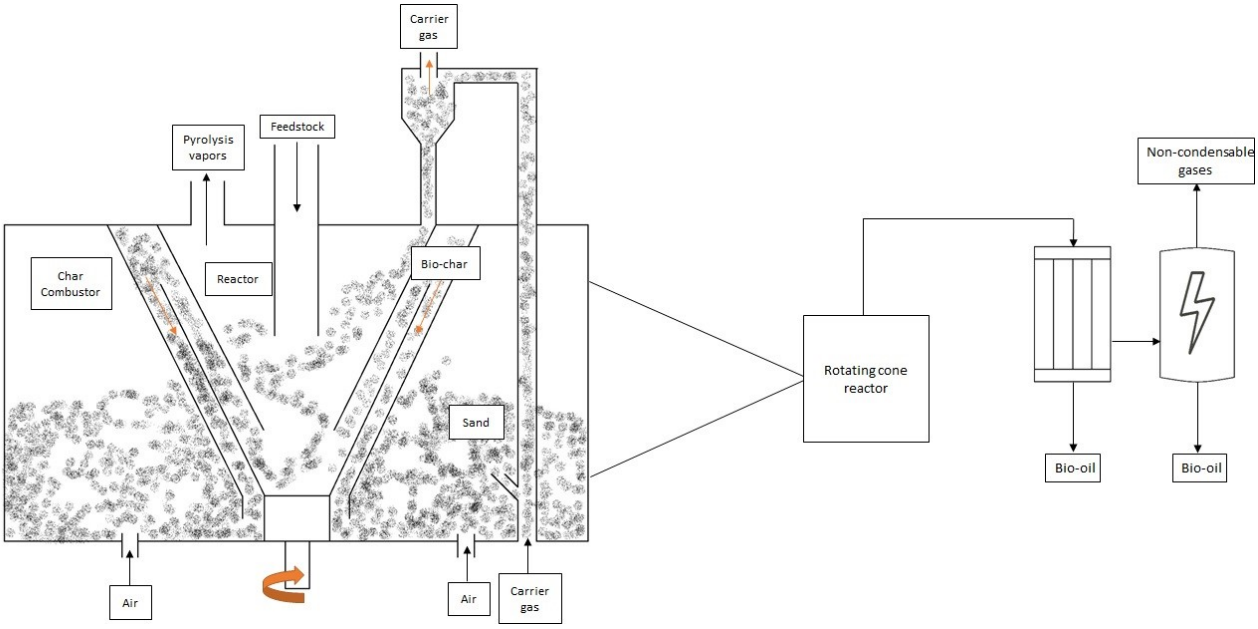

Figure 3: Rotating cone reactor integrated in a typical fast pyrolysis process.
(Figure re-created based on Venderbosch, 2010, San Miguel et al. 2012 and Bridgwater 2012).

2.2.4 Ablative pyrolysis

Ablative reactor consists of a rotating disk; where wood chips are placed under a moving hot plate. The hot surface exerts pressure on biomass to initiate fast pyrolysis reactions. The produced pyrolytic vapours and liquids are carried away by inert carrier gas to be conventionally quenched and collected as bio-oil. The mechanical concept was developed in Aston University. The concept is similar to melting butter by pressing it against a heated pan surface. Ablative reactor is complex in its design, due to the mechanically driven decomposition technique. Figure 4 shows a simplified description of the reactor. Processing relatively large feedstock eliminates the need for a pretreatment stage of biomass milling. Compact design of the reactor is constantly enhanced as the small contact surface is optimized to achieve high heating rates and efficient heat transfer (Bahng et al. 2009). Indirect heating of plates using flue gases at a large scale limits the scalability of this design, due to the small temperature difference between flue gases and reactor, which are 800 °C and 500 °C, respectively (Venderbosch and Prins, 2010). Despite some scalability issues facing

ablative pyrolysis, Pytec has built an ablative pyrolysis plant with a processing capacity of 6 t/d in northern Germany (Bridgwater, 2012).

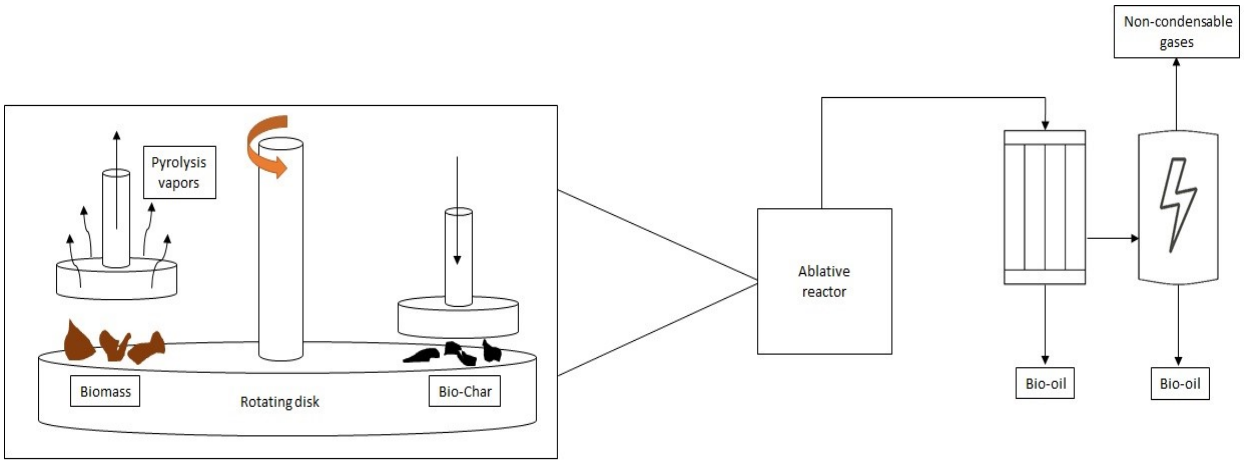

Figure 4: Ablative reactor integrated in a typical fast pyrolysis process.
(Figure re-created based on Venderbosch, 2010, San Miguel et al. 2012 and Bridgwater 2012).

2.3 Innovative integration of fast pyrolysis process.

Integrating fast pyrolysis CFBs into industrial boilers in combined heat and power (CHP) plants exploits multiple revenue streams and converts CHP plants into bio-refineries; where bio-oil is produced alongside heat and power. Based on a patent granted to VTT regarding the integration of a fast pyrolysis CFB with a CHP boiler, Metso (Valmet) co-operated with UPM, Fortum and VTT to integrate a 2 MW_{fuel} fast pyrolysis unit with 4 $MW_{thermal}$ circulating fluidised-bed boiler in Tampere, Finland (Autio et al. 2011). The world's first integrated pilot unit produced 7 t/d of bio-oil. More than a total of 80 tonnes of bio-oil was produced by 2010. Figure 5 shows a flowsheet of the integrated fast pyrolysis unit. Hot boiler sand is used as an efficient heat carrier by circulating it through the reactor. Produced char is separated from pyrolytic vapours and sent directly to the pilot boiler to combust. Pyrolytic vapours are condensed conventionally and collected as bio-oil liquids, and non-condensable vapours are directed back to the reactor and boiler for circulation purposes. Such integration drives down operating costs of running a fast pyrolysis unit and pushes bio-oil production one step towards commercialization.

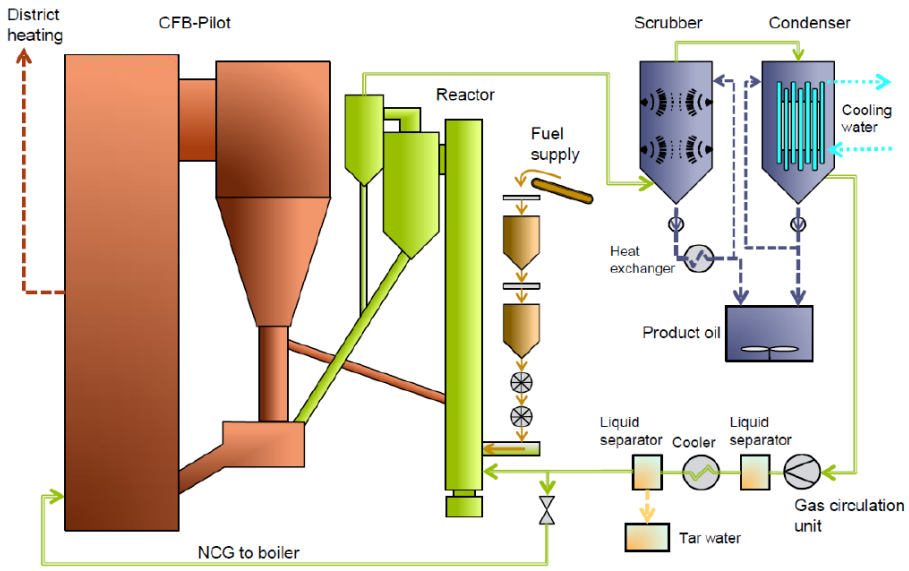

Figure 5: Metso first integrated pyrolysis unit flowsheet (Autio et al. 2011).

As a result of the successful integration of the technology at a pilot-scale, Fortum commissioned world's first commercial scale demonstration unit in 2013. The unit is integrated into combined heat and power production plant located in Joensuu, Finland. 30 MW of oil production is the nominal output of the commissioned plant with a production capacity of 50,000 tonnes annually of bio-oil. The produced bio-oil holds trademark name of Otso™. Otso™ bio-oil is utilized in heat and steam production applications as a substitute for heavy and light fuel oil. Utilizing bio-oil of Joensuu reduces carbon dioxide and sulphur dioxide emissions by 59,000 and 320 tonnes per year, respectively. Figure 6 shows the integration of fast pyrolysis reactor within Joensuu CHP plant. (Meier et al. 2013)

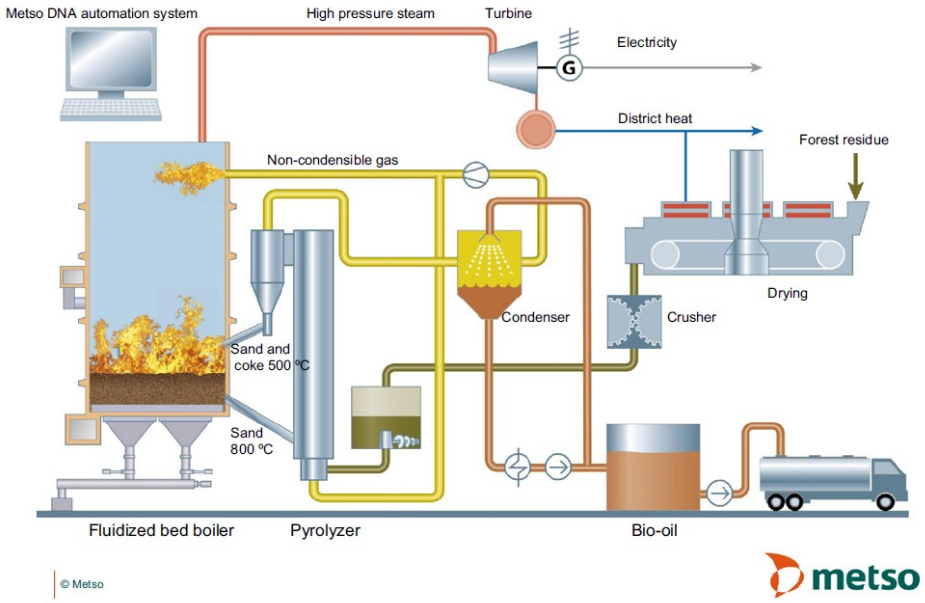

Figure 6: Industrial scale fast pyrolysis plant integrated into CHP plant in Joensuu, Finland (Meier et al. 2013).

2.4 Physio-chemical properties of fast pyrolysis oil

Compared to conventional mineral oil, FPBO is viscous, non-flammable and corrosive liquid with high oxygen and water contents. More than 300 compounds are responsible for the high oxygen content of 35-40 wt. % (dry basis) in bio-oil (Czernik and Bridgwater 2004, Lehto et al. 2013). Studying physio-chemical characteristics is vital for the utilization of bio-oil in different applications. Production of fast pyrolysis liquids is aimed to substitute mineral oils in several combustion applications.

Bio-oils have a distinctive colour of dark brown. However, the colour is dependent on its chemical composition. Char free bio-oils have more translucent red-brown colour. Whereas, bio-oils with high nitrogen content tend to have more of a dark greenish tint. (Bridgwater, 2018)

Instability of bio-oil is observed during product recovery and storage. Phase separation phenomena occurs as a result of feedstock extractives contents of lipids and resin acids. Ageing reactions initiates aqueous phase separation as well. The phase separation often happens when water content exceeds 30 wt. % (Lehto et al. 2013). Biomass containing high level of alkaline metals mainly potassium, tends to reduce organic liquid which induces the phase separation phenomena as a

consequence. Potassium acts as gasification or combustion catalyst by reducing organic liquid yield and by increasing oxidation rates and water formation. In addition, high feedstock moisture content contributes to the severity of phase separation (Agblevor et al. 1995, Lehto et al. 2013). Bio-oils viscosities at 40 °C vary dramatically from 35 to 1000 cP, hinging on biomass and process parameters. Unlike crude oil, bio-oil contains polar and nonpolar compounds. Since FPBO is soluble in semi-polar organic solvents. Methanol, isopropanol and acetone are usually used to reduce bio-oil viscosity significantly (Czernik and Bridgwater 2004). Stability index is used to refer to the change of viscosity inflected by ageing reactions during storage. The index describes the ratio of the change in viscosity during storage to the initial viscosity of freshly produced bio-oil. High index number correlates with low stability bio-oil (Pattiya and Suttibak, 2012).

Ageing reactions also alter the composition of homogenous bio-oil without any increase in its water content, but rather with a change in its water insoluble content. Three fractions are formed while analyzing the chemical composition of bio-oil by solvent fractionation, as shown in figure 7. Diethyl ether is used as a co-solvent in the fractionation process. The three fractions are water-soluble (WS), water-insoluble (WIS) and co-solvent compound fraction as in ether-solubles (ES). WS fraction make up 55 wt. % of bio-oil and consists of water and sugars. Sugars are separated as ethyl insoluble from the WS fraction. 20 wt. % of wet basis bio-oil is made of WIS materials such as, lignin-based materials, extractives and solids. 25 wt. % is made up of co-solvent compounds, such as aldehydes, ketones, mono-phenols, alcohol, light aliphatic acids and aromatic acids. (Oasmaa et al. 2015 a)

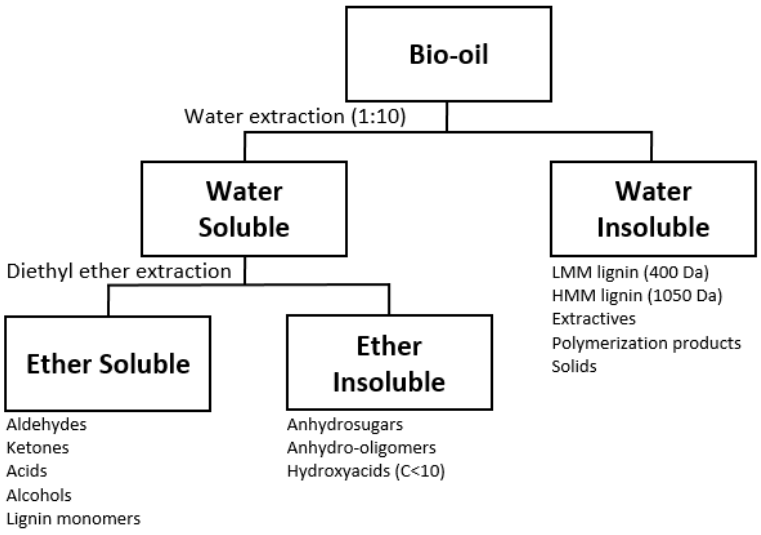

Figure 7: Simplified fractionation scheme (re-created based on Oasmaa et al. 2015 a).

After 1 year of storage time, the composition alters from 55, 20 and 25 wt. % to 55, 25 and 20 wt. % for water soluble, water insoluble and co-solvents fractions, respectively. As shown in figure 8, phase separation began to develop after 2 years with a significant increase in water insoluble content. After 8 years, water insoluble content reached 40 wt. % at the expense of ether-solubles that declined to 5 wt. % (Oasmaa et al. 2015 a). During storage period, water soluble fractions remained relatively constant.

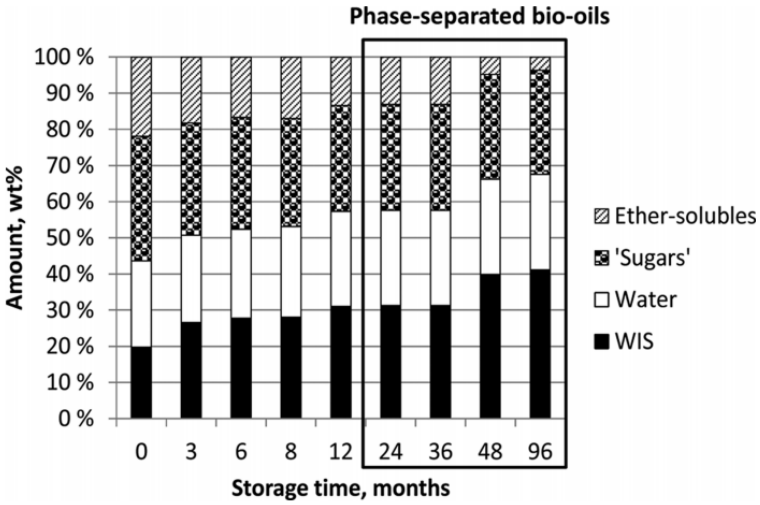

Figure 8: Effect of ageing reactions on bio-oil composition (Oasmaa et al. 2015 a).

Figure 9 shows a ternary-phase diagram of the three different bio-oil fractions. The previously mentioned change in composition can be observed as the freshly produced single phase bio-oil (blue dots) shifts towards the separated phase (red squares) region after 8 years of storage.

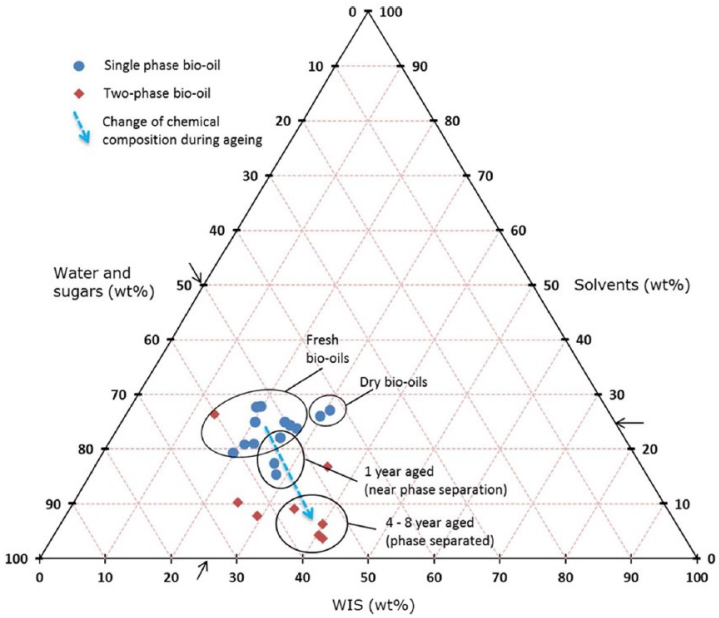

Figure 9: Ternary-phase diagram of different bio-oil fractions indicating phase separation due to storage (Oasmaa et al. 2015 a).

Solids content in water insoluble fraction of bio-oil contribute immensely to the severity of ageing reactions during storage. A typical fast pyrolysis process with a cyclone produces bio-oil with 0.5 wt. % of solids content. Bio-oil solids have a particle size of 5-10 µm, consist mostly of elutriated sand particles and metals alongside some residues of condensed carbon materials (Oasmaa et al. 2005). Sludge layer is formed by accumulation of solids during the storage of FPBO. In addition, downstream equipment and combustion chambers will suffer from erosion and corrosion in the presence of these fine solid particles. Hot vapour filtration method of solid separation showed promising results concerning the reduction of solids content in FPBO (Oasmaa et al. 2005, Lehto et al. 2013). Experimental results regarding this technology will be later discussed in this thesis.

2.5 Fast pyrolysis bio-oils standardization

Several FPBO standards have been approved according to the current legislations and emission standards. American Society for Testing and Materials (ASTM) issued standard specifications for two grades of FPBO; Grade G and Grade D, shown in table 2 (Oasmaa et al. 2015 b). The two grades differ in maximum solids and ash contents. Both grades are not intended to be used in engines, residential heaters or marine applications. However, Grade G is suitable for industrial burners whereas Grade D fits both commercial and industrial burners; due to its low solids and ash contents

(ASTM D7544-12, 2017). Following the European legislations, The European Committee for Standardization (CEN) published specifications of two different grades of fuel that are suitable for industrial boilers (> 1 MW thermal capacity) (CEN – EN 16900). CEN also issued a technical report about some of the acceptable qualities of FPBO for internal combustion engine (ICE) applications. No fuel specifications were agreed on; due to the lack of data concerning the commercialization of FPBO for ICE applications (CEN-TR 17103). CEN is working on publishing two other FPBO technical specifications; they are regarding the utilization of FPBO as a gasification feedstock, and the co-processing of FPBOs with mineral oils in refineries (CEN-TR 17103). Reducing oxygen, solids, ash and AAEM contents of FPBO are necessary to valorize FPBO into transportation fuels. Chapter 3 include the necessary chemical and physical upgrading methods for such a valorization.

Table 2: ASTM fuel grades for FPBO (Oasmaa et al. 2015 b).

Property	Grade G	Grade D
Gross heat of combustion, min (Mj/kg)	15	15
Water content, max (mass %)	30	30
Pyrolysis solids content, max (mass %)	2.5	0.25
Kinematic viscosity at 40 °C, max (mm^2/s)	125	125
Density at 20 °C (kg/dm^3)	1.1-1.3	1.1-1.3
Sulfur content, max (mass %)	0.05	0.05
Ash content, max (mass %)	0.25	0.15
pH	Report	Report
Flash point, min (°C)	45	45
Pour point, max (°C)	-9	-9

3. Upgrading technologies

Current industrial projects such as Otso™ bio-oil have already achieved feasible substitution of fossil-based oil in heat and steam generation applications. However, transportation fuel market has various challenges, due to the unstable characteristics of FPBO. Upgrading bio-oil is required to match the current transportation fuel market specifications. Upgrading methods are aimed to remove oxygen content, in addition to minimize bio-oil viscosity, solids content and impact of ageing reactions. Upgrading methods are mainly categorized into chemical and physical upgrading technologies.

3.1 Chemical upgrading

Chemical upgrading technologies rely mainly on promoting certain reactions by adjusting process parameters or by introducing a certain catalyst to achieve better final product properties. Chemical upgrading technologies include hydrodeoxygenation, zeolite cracking, hydrothermal treatment and esterification.

3.1.1 Hydrodeoxygenation

Hydrodeoxygenation (HDO); commonly known as hydrogenation or hydrotreatment, is a catalytic upgrade process for the reduction of oxygenates in bio-oil. Hydrogen is used to reduce oxygenated compounds by forming water as a product. HDO oil have high heating values analogous to crude oil (Mortensen et al. 2011). Series of reactions occur during hydrodeoxygenation, such as hydrogenation (saturation of C=O and aromatic rings), hydrodeoxygenation (C-O cleavage), decarboxylation (carboxyl group cleavage), hydrogenolysis (C-C and C-heteroatom cleavage), hydrocracking (C-C cleavage) and dehydration. High pressure (> 200 bar) and temperature (400 °C) are needed to favor deoxygenation reactions and achieve optimum balance among these reactions (Sharifzadeh et al. 2019). Figure 10 shows the overall HDO chemical reaction. Single stage of HDO imposes challenges such as, excessive coke deposition and low yield of organic liquids. Researches from Pacific Northwest National Laboratory (PNNL) proposed two-stage hydrotreatment process to promote hydrogenation and reduce coke deposition (Elliot and Baker, 1989). The two stages consist of an oil stabilizing step to hydrotreat reactive compounds followed by deoxygenation step. Bio-oil yields increased from 23 wt. % to 30-50 wt. % with 1% oxygen content. However, coke formation

remained an issue. PNNL collaborated with Battelle and developed a new process with better catalyst regeneration. This process includes ion exchange; to clean up bio-oil prior to the two-stage hydrotreatment process. They claimed stable catalyst regeneration for over 1000 h (DOE. 2015, Si et al. 2017).

$$CH_{1.4}O_{0.4} + 0.7\,H_2 \rightarrow 1"\,CH_2" + 0.4\,H_2O$$

Figure 10: Overall HDO reaction (Mortensen et al. 2011).

3.1.2 Zeolite cracking

Zeolite cracking is an alternative method for removing oxygen content, by using zeolite catalysts (e.g. HZSM-5). Hydrogen is not required for this process, which makes it an economically viable option. However, zeolite cracking oil is regarded as lower grade than HDO oil, and has lower heating values than crude oil. Like HDO, similar set of catalytic reactions occur in zeolite cracking, favoring cracking reactions to decrease oxygen content. An overall reaction is shown in figure 11. Since no additional hydrogen is utilized in zeolite cracking, oxygen is removed as CO, CO_2 and H_2O. Unlike HDO, where oxygen is predominantly removed as water. Cracking rate is controlled within a temperature range of 400-550 °C. Higher temperatures will degrade oil to light gases and carbon (Mortensen et al. 2011). Coke formation appears to be an issue over HZSM-5. However, continuous regeneration in an in-situ catalytic fast pyrolysis process is possible by circulating catalyst alongside sand through the combustor in a circulating fluidised bed configuration (Paasikallio, 2016).

$$CH_{1.4}O_{0.4} \rightarrow 0.9"CH_{1.2}" + 0.1\,CO_2 + 0.2\,H_2O$$

Figure 11: Overall zeolite cracking reaction (Mortensen et al. 2011).

3.1.3 Hydrothermal treatment

Hydrothermal upgrading (HTU), well known as aqueous processing of FPBO, is an effective deoxygenation method. 30% of hydroxyl groups are deoxygenated in a short amount of time (< 30 min). In hydrothermal upgrading, FPBO is mixed with water at near-supercritical or supercritical conditions (300-400 °C and <200 bar). At 300 °C, compressed hot water act as acetone in terms of

polarity order and dissolves bio-oil producing single deoxygenated phase. Despite low deoxygenated oil yield of HTU, carbon dioxide and large amounts of hydrogen are produced as co-products (Sharifzadeh et al. 2019). Hydrothermal treatment step prior to hydrodeoxygenation step is a viable option; since the produced hydrogen from HTU can be utilized in HDO. The synergistic integration also reduces the hydrogen requirement in HDO, since significant amounts of oxygen have been already removed in the former stage of HTU (Sharifzadeh et al. 2015). Such integration reduces fuel price dramatically.

3.1.4 Esterification

FPBO is highly corrosive and characterized with low energy content due to the presence of highly reactive oxygenated compounds, such as carboxylic acids, aldehydes and ketones. Esterification of bio-oil is an effective method for converting undesirable acids and aldehydes into esters and acetals, respectively, as shown in figure 12. Utilizing water soluble alcohol, such as methanol, requires water removal prior to esterification. Whereas, utilizing water insoluble alcohol, such as n-butanol, demands water removal during esterification to avoid reverse reactions (Sundqvist et al. 2015). The upgrading method involves mild heating (60-120 °C) and adding alcohol (30-100 wt. %) to bio-oil. Esterification differs from the conventional method of upgrading bio-oil with alcohol by employing homogenous or heterogeneous catalyst, eventually achieving complete neutralization of acidity.

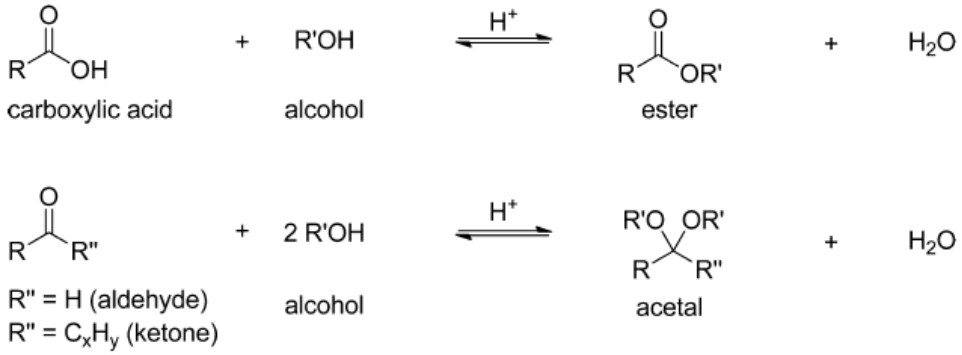

Figure 12: Reaction pathways of FPBO reactive compounds reacting with alcohols (Sundqvist et al. 2015).

Several homogeneous and heterogeneous catalysts were investigated by Sundqvist et al. (2015) Amberlyst-15 (heterogeneous commercial catalyst) has been tested with bio-oil and methanol (2:1

wt. %) and resulted in bio-oil with low total acid number (TAN) of 10 mg/g and slight increase of pH value from 3 to 4. They also tested P-toluenesulfonic acid (p-TSA) as a homogeneous catalyst with 90% of n-butanol. Upgraded bio-oil had a TAN of 5 mg/g and a pH value of 5.5. Azeotropic distillation steps were implemented prior and during esterification, while using methanol and n-butanol, respectively (Sundqvist et al. 2015). Esterified bio-oils have relatively higher energy content and are less corrosive than normal bio-oils. They are best utilized in specific applications, such as robust combustion engines.

3.2 Physical upgrading

Influencing the final product stability can be done by adjusting the physical constituents of either feedstock, mid-process products or final products. This section will cover different physical upgrading methods that alter the physical constituents of bio-oil e.g. ash and solids content. The physical upgrading technologies include pretreatment of biomass, liquid and hot vapour filtration.

3.2.1 Pretreatment of biomass

Removal of solid particles (e.g. ash and metals) is an essential upgrading method, due to their obstructive effect on bio-oil (mentioned in section 2.4). Presence of ash, alkali and alkaline earth metals promote ageing reactions and induce aqueous phase separation. These components are considered harmful for downstream equipment as well. Several thermal and washing pre-treatments are considered for fast pyrolysis (Liu et al. 2017). Thermal pre-treatments concerning the reduction of ash and metals are hot water extraction and steam explosion. Whereas, washing pre-treatments include water and acid washing.

3.2.1.1 Thermal pre-treatment

Hot water extraction (HWE) is one of the effective thermal pretreatments for biomass. The chemical free process is conducted at relatively moderate temperature (120-260 °C) (Liu et al. 2017). Liu et al. (2017) studied the influence of hot water extraction on several inorganics and metals; among them alkali and alkaline earth metals (AAEM) (e.g. K, Mg and Ca). Switchgrass and pine bark were extracted by hot water. For switchgrass biomass, 99% of potassium was removed alongside 83% of magnesium and 13% of calcium. Whereas, for pine bark, 67% of potassium, 51% of magnesium and 34% of calcium were eliminated from the end product. Decent removal efficiency is due to the

solubility of alkali metals in water. Furthermore, ash reduction during several extraction experiments was temperature dependent, with highest reduction of 69.6% and 73.3% for switchgrass and pine bark, respectively (Liu et al. 2018).

Steam explosion (SE) is one of the widely implemented thermal pre-treatment upgrades for biomass at commercial scales. The process involves pressurizing biomass with saturated steam at around 70 bar; where steam effectively cracks hemicelluloses and increases lignin content. Biswas et al. (2011) examined the effect of steam explosion on Salix wood chips. They noticed a reduction in ash content from 2.4% to 1.8% (dry basis), alongside a significant reduction of sodium and potassium contents close to 50%. (Biswas et al. 2011)

3.2.1.2 Washing pre-treatment

Various washing pre-treatment methods have been investigated for inorganic reduction of ash and AAEM. Water and acid washing methods were the most common and effective ones. Washing techniques optimize FPBO and alter its final composition by reducing ash and AAEM content.

Stefanidis et al. (2015) studied the influence of water and acid (nitric and acetic acid) washing on inorganic contents and on bio-oil yield of different energy crops, forestry and agricultural residues. Acid washing experiments proved that nitric acid is more suitable than acetic acid. Stefanidis et al. (2015) reported 42% and 90% inorganic removal for water and acid washing experiments, respectively. According to the results, washing temperature affects significantly the final outcome. High temperature washing (50 °C) is more effective than washing at room temperature for both washing techniques. In addition, higher bio-oil yields were reported for the pre-treated biomass. However, a relative increase in bio-oil oxygen content was observed alongside a reduction in lignin-derived compounds.

3.2.2 Liquid filtration

Filtration of solid particles from pyrolysis liquids is a post-treatment technique. Bio-oil filtration is faced with several challenges, such as the insignificant removal efficiency of soluble AAEM, the need for additional equipment for the disposal of generated sludge, and the long filtration time due to the high viscosity of FPBO at room temperature. (Liao et al. 2013)

Microfiltration technique of bio-oil has been developed by Javaid et al. (2010) to overcome these challenges. Tubular ceramic membranes with nominal opening sizes of 0.5 and 0.8 µm were used to achieve effective removal of solid particles from bio-oil. Process temperature and pressure ranges from 38 to 45 °C and from 1 to 3 bar, respectively. The pressure gradient is across 3 different trans-membranes (Javaid et al. 2010). Efficient membrane cleaning technique was implemented, using methanol, sodium hydroxide and acetic acid. Removal of char particles (>1 µm) was achieved by this technology with significant reduction in ash content. However, bio-oil ageing process was not improved despite the removal of char particles. Microfiltration still needs a lot of research and it is not considered a practical upgrading method at large scale applications.

3.2.3 Hot vapour filtration

Hot vapour filtration (HVF) is conducted at temperatures above 260 °C. HVF unit of fast pyrolysis is based on hot gas filtration technology; a technology that has been part of either pressurized fluidised-bed combustion (PFBC) or integrated gasification and combined cycle (IGCC). The technology protects downstream equipment from particle contaminants. These particles causes fouling and erosion in the short and long run (Alvin, 1998). Unlike pre-treatment methods (acid and water washing) or post-treatment method of liquid filtration, HVF upgrades pyrolytic vapours mid-process. Significant improvement in bio-oil stability is achieved by implementing hot vapour filtration method. HVF reduces bio-oil solids content; by removing char and inorganic particles prior to the quenching stage in fast pyrolysis. Efficient removal of char eliminates the additional costs for expensive liquid and flue gas treatment systems (Heidenreich, 2013).

Agglomeration of char contributes to the upgrading of bio-oil, by promoting secondary cracking of vapours, leading to a reduction in viscosity of bio-oil. Char fines and AAEM have the ability to catalytically crack high molecular weight compounds (Pan and Richard, 1989). Recent studies and development regarding the process will be discussed thoroughly in section 4.

4. Hot vapour filtration

4.1 Principle

Hot vapour filtration unit consists of porous and permeable filter elements with one closed end to direct the flow of vapours. Filters are made of ceramic, or metal elements for high temperature applications. During filtration, untreated vapours permeate the porous filter candles, where dust and micro-size particles attach to the surface of the candle. Treated clean vapours proceed to exit the filter through the open end. During operation, dust particles agglomerate and form a thick layer covering the candles, called dust cake. Formation of cake creates a barrier between untreated and clean vapours. This barrier increases pressure difference, as a consequence. Pressure regeneration techniques such as reverse jet pulse of pressurized gas and controlled oxidation, are used to detach the cake and reduce pressure difference across the filter. (Heidenreich, 2013)

In vapour filtration, char fines and AAEMs are filtered by two filtration mechanisms; surface and depth filtration. Separation of particles larger than pore size is achieved through surface filtration; where particles are attained on the surface of the filter by a sieving mechanism. Resulted cake can be removed during operation with jet pulsing techniques. Whereas depth filtration or inertial impaction occur inside the porous filter media; where finer particles are captured by diffusion. Removing the filter medium is needed for cleaning the captured particles through depth filtration. (Rubow et al. 2006)

Designing an efficient HVF system requires an adequate knowledge of particle size distribution, and suitable face velocity. Face velocity describes vapour flow rate per unit filter area (Rubow et al. 2006). The filtering area in a filtration unit is designed based on the utilized flow rates of vapours (Aroussi et al. 2001). Premature blinding of filter elements is typically caused by high face velocities. Decent filter cake formation enhances filtration efficiency. Filter cake porosity is directly proportional to particle sizes and inversely proportional to particle densities and face velocities. Integration of HVF technology into a fast pyrolysis process is a challenging task. An efficient cake removal technique is required, since early condensation of vapours inside the filter forms a sticky cake. This cake is hard to remove. Plugging the porous surface with the cake eventually leads to permanent blinded filters (Solantausta et al. 2001).

4.2 Hot vapour filtration systems

In solid separation applications, cyclones are commonly used at industrial scale. However, the separation of fine particles is not efficient in typical cyclones. Cyclones separate large particles (> 10 µm) and large liquid droplets (Liao et al. 2013). Their collection mechanism relies on inertial forces; by employing centrifugal forces inside the unit (Jung et al. 2004). Different filtration systems have been introduced for better control of temperature, pressure drop and residence time of vapours inside the unit. Cake formation imposes many challenges for every design such as filters blinding and cake bridging. Blinded filters are common; as a result of dense cake formation, while bridging occur when cake grow and connect with other filter candles or with the wall. Cake bridging causes tensile forces, resulting in the breakage of candles. Depending on the filtration system, different techniques are employed for efficient cake removal.

4.2.1 Baghouse filter

Baghouse vessel design holds single (tube-sheet) or multiple stage designs of different filter elements. Figure 13 shows a scheme of the most commonly used single stage baghouse equipped with reverse jet pulse regeneration system. In a fast pyrolysis setup, pyrolytic vapours enter the baghouse from the bottom through filter elements, and exit from the top as filtered vapours. The solids content agglomerates over the outer surface of the elements creating char cake. Cake regeneration is done by bursting inert gas through filter elements to detach the cake.

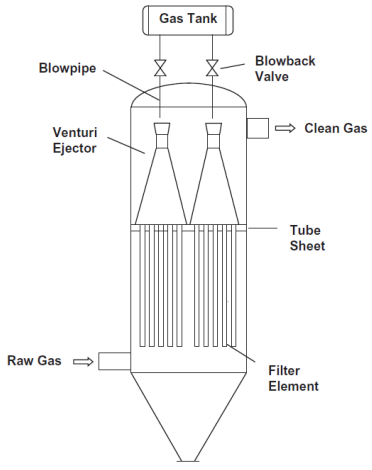

Figure 13: Scheme of a typical baghouse with single tube-sheet design (Heidenreich et. al. 2013).

Multi-stage filtration vessels were first designed by Lurgi Lentjes Babcock (Heidenreich, 2013), shown in figure 14. The filter elements are erected on manifolds at different levels, instead of hanged as in single stage design. The resting weights of filter elements on manifolds assure constant compression and therefore better durability since in multi stage design, filter elements are less likely to break compared to the conventional hanged design (Heidenreich et. al. 2013). Raw vapours enter from the top and pass through filter candles and then dispatch from the sides. The multi-stage design is equipped with reverse pulsing regeneration technique. This technique blows solids off the surface of the candles to be collected from the bottom.

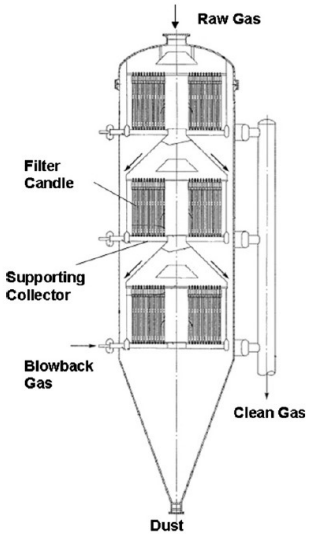

Figure 14: Scheme of a baghouse with multi stage filter candles design (Heidenreich et. al. 2013).

4.2.2 Moving granular bed filter

Moving granular bed filter (MGBF) is one of the promising technology for hot vapour filtration applications. The moving granules function as a filtering medium for solid separation. Cake formation occur over granular particles surface as a results of interacting with particle-laden vapours. Thickness of cake influences filtration efficiency. As reported by Chen and Hsiau (2009), 1 mm of cake thickness enhances solid collection by 0.686% (Chen and Hsiau, 2009). High filtration efficiency of 99.9% was achieved for particles > 1 µm, by employing MGBF as a filtration unit. Furthermore, soaring collection efficiencies of 84% and 96% were achieved for submicronic particles (Abatzoglou et al. 2002). Several designs have been introduced. They are categorized according to the flow direction of process vapours relative to the moving granules. Figure 15 shows the two most common moving granular beds; cross-flow and counter-flow granular moving bed, in figure 15(a)

and figure 15(b), respectively. In cross-flow granular moving bed, vapours are passing the bed perpendicular to the moving granules. This specific design of cross-flow granular moving beds was developed by Hsiau et al. (2004). The louvered-wall is designed to assure symmetric flow of material in the middle, and the central saddle roofs function as flow corrective plates to eliminate quasi-stagnant zones and assure effective movement of the materials (Hsiau et al. 2004). Counter-flow granular moving bed was introduced by Brown et al. (2003). Particle-laden vapours travel upward to the opposite direction of granular materials flow. Dip-leg flow of granules is straightened by the positioned stators in the bottom part of the filter. The existing screen in the design prevents the backflow of granules with clean vapours stream in case of high vapour flow rates (Brown et al. 2003). In counter-flow design, cake is constantly regenerated and dispersed by the fresh moving granules. In addition, particle-laden vapours are initially filtered by cake-stained granules; allowing porous cake to enhance the filtering efficiency.

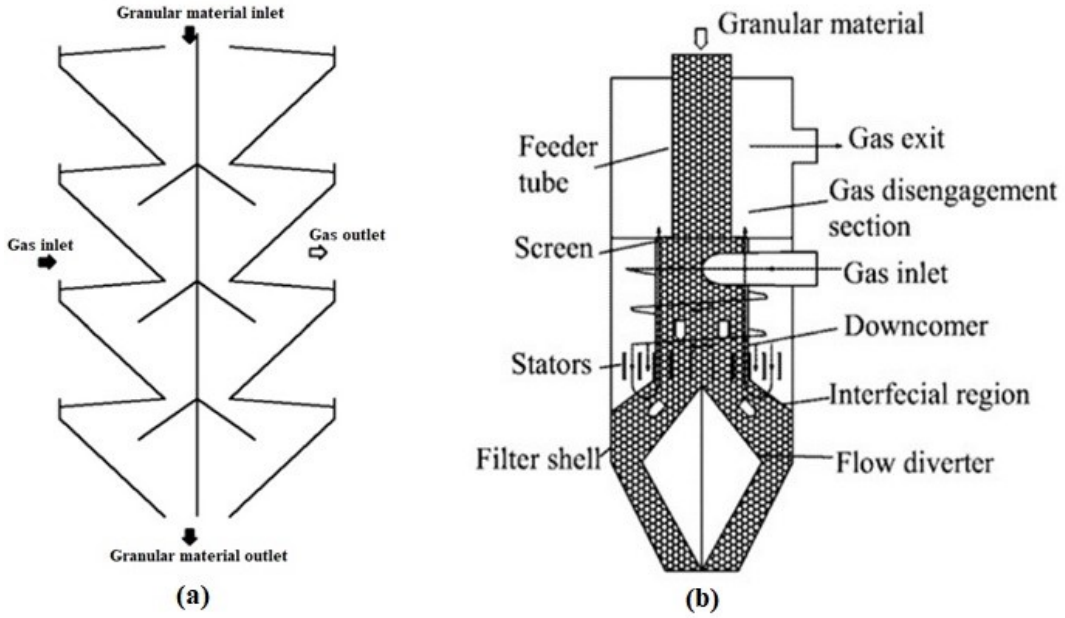

Figure 15: Moving granular bed filters, (a) cross flow granular moving bed, (b) counter flow granular moving bed (Xiao et al. 2013).

In addition to the previously mentioned designs, co-current filters have similar designs to the counter-flow filters. However in co-current flow, the stained granules are in direct contact with the freshly filtered vapours (Xiao et al. 2013). Continuous operation of MGBF is possible, however several equipment are needed for handling high throughputs of granules.

4.3 Filter media

Filtering elements in hot vapour filtration process require mechanical stability which is governed by mechanical strength, degradation rate, elasticity, and absorption at the material interface.

4.3.1 Ceramic filter media (Baghouse)

High and low density ceramics are used as filter media. High density filter media are made of sintered particles of silicon carbide, alumina or cordierite with 40% porosity. Whereas, low density ceramics are usually made of alumosilicate fibres with high porosity of 90% (Heidenreich, 2013). Regenerative back pulsing intensity should be managed to avoid the release of fibres, especially from low density filter media, that exhibit low differential pressures during operation. Ceramic elements can withstand up to 1000 °C of process temperature. However, reliability of ceramic filters above 815 °C is concerning, due to chemical degradation and high possibility of a fatigue failure (Cummer and Brown, 2002).

4.3.2 Metal filters media (Baghouse)

Metallic filter media are typically utilized in high temperature gradient applications, due to their high thermal conductivity. Metallic filters are made of sintered metal or metal alloy. Sintered metal elements are manufactured by sintering fibre or powder metals in hydrogen or under vacuum. Fibre and powder based metals media have porosities up to 90% and 40%, respectively. Different metal alloys are also employed, such as stainless steel and high temperature steel. Special metal alloys such as Inconel, Monel or Hastelloy are typically used for high temperature gas applications containing sulphur or chloride. (Heidenreich, 2013)

4.3.3 Granules (MGBF)

Variety of materials can be used as MGBF media depending on the application. Granular materials must be selected carefully for high temperature filtration processes. Granule temperature resistance plays an important role in stabilizing the process and avoiding side reactions. Physical properties of MGBF media is of utmost importance. Granular materials must endure mechanical strains and resist attrition and corrosion. In addition, granules need to be selected according to their ability to withstand various thermal gradients (Xiao et al. 2013). Silica sand and glass beads have

been used by Chen et al. (2009 and 2012) in their cross-flow and counter current MGBFs, respectively. Both of these filters were operating at room temperature. (Chen et al. 2012 and 2009)

4.4 Filtration temperature

Understanding the impact of filtration temperature on products composition is necessary to maximize the yield of bio-oil. Paenpong and Pattiya (2016) investigated the effect of both pyrolysis and filtration temperatures on products yields, as shown in figure 16. The experimental fast pyrolysis unit consisted of a fluidised bed, primary cyclone and a moving-bed granular filter. Granular filter temperature kept constant at 380 °C; to investigate the influence of pyrolysis temperature on product distribution and decide the optimum pyrolysis temperature. As they increased pyrolysis temperature from 400 °C to 500 °C, organic and gas yield increased at the

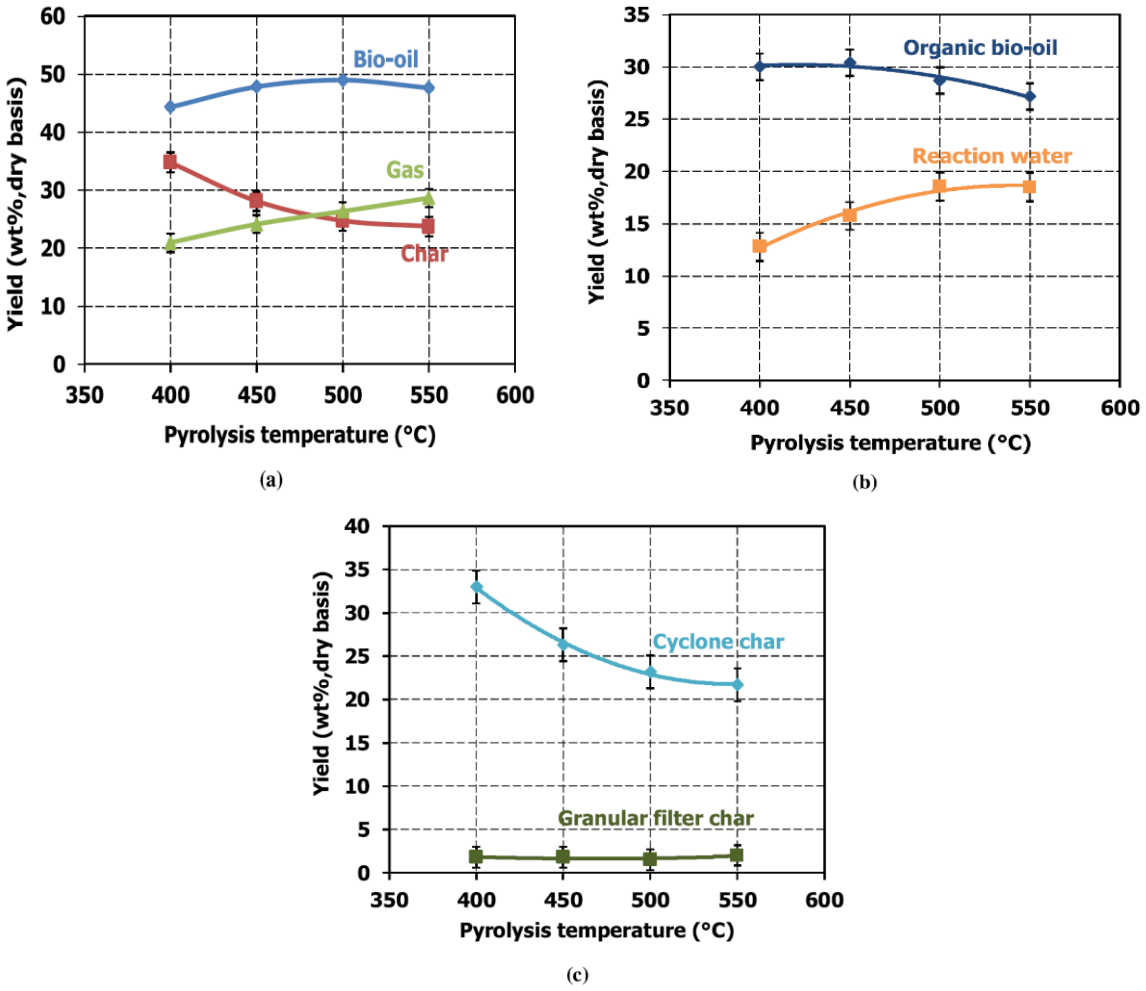

Figure 16: Pyrolysis temperature influence on (a) bio-oil, gas and char yield, (b) organic bio-oil and reaction water and (c) the yield of cyclone and granular filter chars (Paenpong and Pattiya, 2016).

expense of char yield. Further increase of temperature to 550 °C increased the gas yield as the organic yield decreased. Char decreased slightly as the temperature increased above 500 °C, it can be shown in figure 16 (a). Figure 16 (b) shows the yield of organics and reaction water in bio-oil. Reaction water increased as pyrolysis temperature increased, whereas the organic part of bio-oil remained constant between 400 and 450 °C, which indicates that reaction water was the product of biomass decomposition rather than organics cracking. Further increase of temperature to 550, decreased Organic yield of bio-oil. Figure 16 (c) illustrates the yield of char from cyclone and granular filter. Cyclone char yield decreased as reaction temperature increased. The calculated filtration efficiency of granular filter ranged between 92.3% and 94.5% as pyrolysis temperature increased from 400 to 550 °C. Paenpong and Pattiya (2016) concluded that 500 °C is the optimal reaction temperature; to achieve a maximum yield of 49 wt% from pyrolysing cassava rhizome in the fluidised-bed. Moreover, filtration efficiency of the granular filter was not significantly impacted by the different reaction temperatures (Paenpong and Pattiya, 2016).

After setting pyrolysis temperature to 500 °C, Paenpong and Pattiya (2016) manipulated granular filter temperature to study its impact on product distribution. As shown in figure 17 (a), as the temperature increased from 350 °C to 380 °C, char decomposed to bio-oil. Char yield decreased from 28.6 to 26.4 wt. % and bio-oil yield increased from 45.4 to 48.9 wt. %. Gas yield increased slightly from 26.0 to 26.4 wt. %. Insignificant change in products yields as filtration temperature increased to 410 °C. Figure 17 (b) shows that slight reduction of organics in bio-oil happened as the filtration temperature increased from 350 to 380 °C. Reaction water in bio-oil increased due to organic cracking. In addition to that, the declining trend of cyclone char in figure 17 (c) indicates the contribution of char to the production of reaction water. Trends suggest that the decomposition of char to organics might have been followed by dehydration of organics, which resulted in an increase in the production of reaction water and gases, as shown in figure 18 (Paenpong and Pattiya 2016). Alongside the conventional pyrolysis vapour cracking, char secondary cracking contributes to the production of organics, reaction water and permanent gases. In addition, dehydration of organics at filtration temperatures between 350 and 380°C produces reaction water and gases as well. (Paenpong and Pattiya 2016)

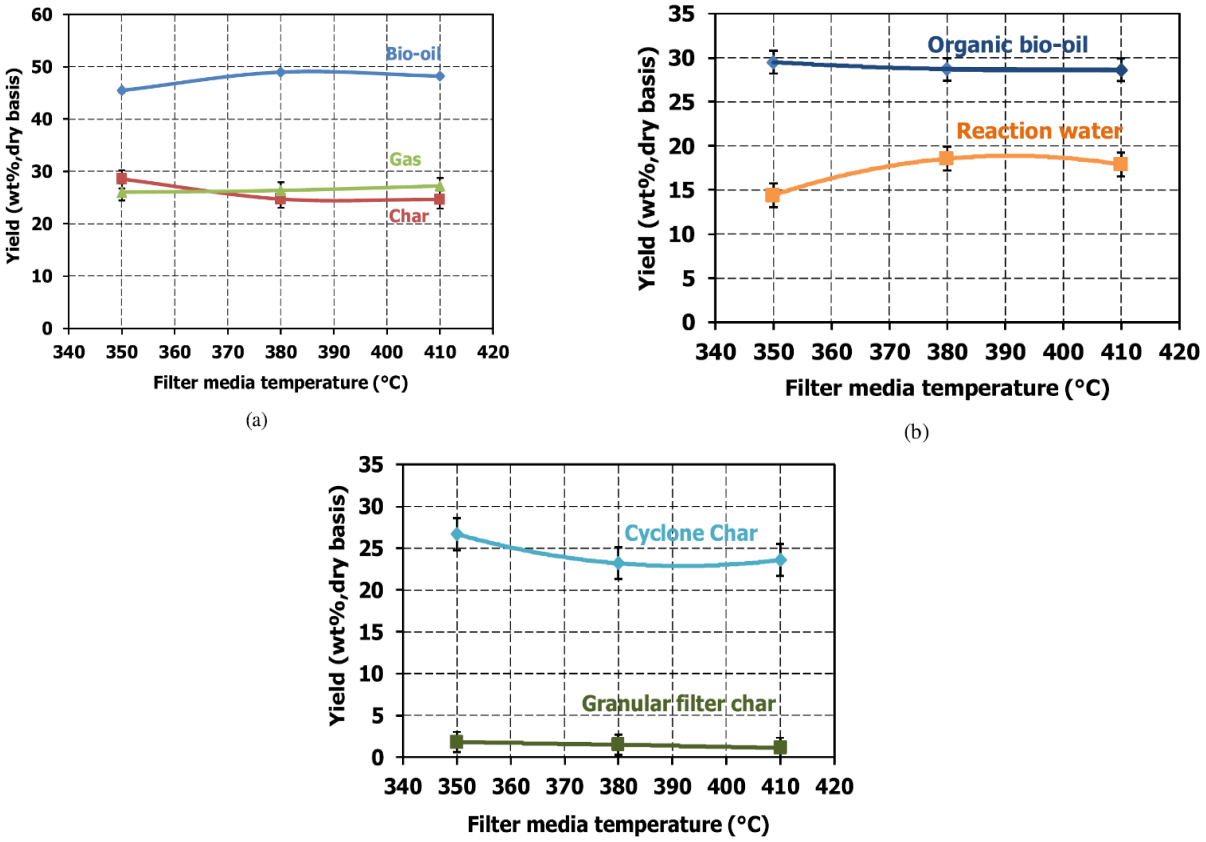

Figure 17: Filtration temperature influence on (a) bio-oil, gas and char yield, (b) organic bio-oil and reaction water and (c) the yield of cyclone and granular filter chars (Paenpong and Pattiya, 2016).

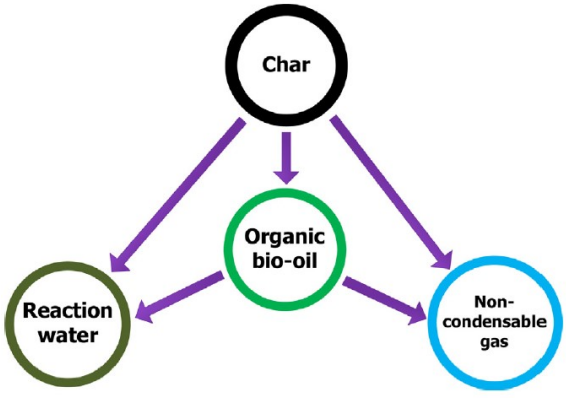

Figure 18: Potential reactions at hot vapour filtration temperatures between 350-380 °C (Paenpong and Pattiya, 2016).

Mei et al. (2016) investigated the changes of pyrolytic product yields and properties with and without HVF unit. Different HVF temperatures ranging from 350 to 500 °C were tested. Ceramic hot

vapour filter was used to filter the pyrolytic vapours that are produced from pyrolysing pine sawdust in a fluidised-bed reactor. They witnessed similar reduction trend in bio-oil yield as they incorporated the HVF unit; due to the additional residence time which promotes thermal cracking of vapours. The highest yield of filtered bio-oil was obtained at a filtration temperature of 400 °C whereas the lowest yield was obtained at 500 °C. Owning to the Boudouard gas reaction at high filtration temperatures, the non-condensable gases (NCG) yield increased as HVF temperature increased from 350 to 500 °C. However, the composition of NCG stayed relatively the same at different filtration temperatures. The highest bio-char yield was generated at low filtration temperature of 350 °C. The results showed an inversely proportional relationship between bio-char yield and the different filtration temperatures. The study concluded that formation of NCG contributes mainly to the reduction of the filtered bio-oil yield. (Mie et al. 2016)

4.5 Research and development

This section will highlight the results of different hot vapour filtration experiments in several research institutes and universities.

4.5.1 National Renewable Energy Laboratory (NREL)

NREL initially tested the effect of hot filtration on pyrolytic vapours to overcome the formation of coke over zeolite (ZSM-5) catalyst. ZSM-5 was used to produce aromatic gasoline (Diebold and Scahill, 1988). A filtration system was integrated with a vortex ablative reactor. Sintered Inconel filters (2 and 5 µm) were used at 400 °C. Successful collection of char fines circumvented the deteriorating coke formation over the catalyst.

NREL initiated series of experiments regarding the upgrading technology. Starting with the addition of baghouse filter unit to their vortex ablative reactor. The commercially manufactured stainless steel baghouse unit has four filters, and it is equipped with reverse jet pulse regeneration technology. Baghouse has a filter surface of 1 m^2, and ability to process 1.7 m^3 of gas flow rate at 3-6 seconds of vapours nominal residence time (Diebold et al. 1995). Conducted experiments proved the practicalities of controlling pressure drop across the filter. In addition, char fines were observed as the main source of alkali content in FPBO, despite the imprecise alkali content analytical techniques used at that time.

Further progress has been achieved regarding process optimization through series of experiments. NREL experiments were set to adjust pyrolysis severity in vortex reactor and cracking severity in baghouse unit (Diebold et al. 1996). The aim was to attain high oil yields by maintaining low operational temperature inside the filtration unit. Investigating different operational parameters and setups resulted in optimal bio-oil yields and minimal ash and alkali content in the final product. High bio-oil yield was achieved by placing two cyclones prior to the baghouse. The implemented configuration reduced baghouse operational temperature, by extending vapours residence time inside the two cyclones before reaching the filtration unit. Only char fines are directed to the baghouse. Sintering of char fines resulted in a relatively thinner but denser cake. (Diebold et al. 1996)

Efficient removal of char cake was also investigated by NREL. Effective removal of filter cake becomes a challenge for a continuous process, due to char fines sintering over the surface of the filter. Controlled oxidation was inspected as a potential regeneration method (Scahill et al. 1997). The experimental setup of two cyclones and a baghouse was adjusted by removing the two cyclones prior to the baghouse; to avoid dense cake formation. NEXTEL^{TM} ceramic fibre cloth bags with a nominal pore size of 2 μm were used. Cloth bags can withstand temperatures up to 760 °C. Successful regeneration was achieved after 6-9 hours of controlled oxidation at 600 °C. However, ash residues formed over the fabrics; as a result of char oxidation. Ash residues are catalytically active, they lead to faster filter blinding by converting pyrolytic vapours into char. Controlled oxidation was not recommended for regeneration purposes after this experiment, and further research regarding cake formation was demanded to develop an efficient cake removal technique. (Scahill et al. 1997)

In 2002, NREL collaborated with Enerkem and Université de Sherbrooke to develop a novel moving granular bed filter (NMGBF) (Abatzoglou et al. 2002). First set of experiments was aimed to establish and optimize the operating conditions for a cold and dry experimental model of the NMGBF. In the second experimental study, prototype of the model was built and installed in a gas cleaning train of a gasification system. The downward moving bed had a velocity between 2.54 and 3.81 cm/h. The pressure drop across the filter was more stable with a moving bed than with a fixed bed. The hot

NMGBF exhibited high filtration efficiency of 99.9% for particles larger than 1 μm, and between 84% and 96% for submicronic particles. (Abatzoglou et al. 2002)

NREL investigated bio-oil stabilization as well, by testing two different filter elements; porous sintered stainless-steel (PSS) and sintered ceramic powder filter elements (Baldwin and Feik, 2013). Filter unit containing those elements was attached to a slipstream of NREL 0.5 MTD vortex reactor process development unit (PDU). Experimental results showed a reduction in the upgraded bio-oil yield of 10-30 wt. % over the tested filter elements. PSS filtered bio-oil did not pass the U.S. Department of Energy (DOE) ageing test. The ageing test measures viscosity increase rate at 80 °C to simulate long storage conditions for the obtained bio-oil. On the other hand, ceramic filtered bio-oil passed the DOE ageing test. Both filters produced bio-oil low in AAEMs and solids content, however PSS filtered bio-oil contained high iron content. (Baldwin and Feik, 2013)

4.5.1.1 Collaboration with Pacific Northwest National Laboratory (PNNL)

NREL collaborated with PNNL to investigate the effect of catalytic hydroprocessing of different hot vapour filtered bio-oils. Feedstocks of oak and switchgrass were tested (Elliott et al. 2014). The experimental setup included a cyclone for char removal prior to the HVF unit. 2 μm stainless steel filter elements were used. PNNL two-stage catalytic hydrotreatment process included two fixed beds with sulfided Ruthenium on carbon catalyst and sulfided CoMo on alumina catalyst in stage 1 and 2, respectively. Stage 1 catalyst operated at 220 °C and 100 bar, whereas alumina based catalyst was active at 400 °C with the same operating pressure. Several results were obtained from the analysis of four 1 liter samples of filtered and unfiltered bio-oils from oak and switchgrass feedstocks. 10% reduction in fuel yields was observable for the filtered products with higher gas yields. Ca and K contents were reduced by 98% for the filtered switchgrass-based bio-oil. Whereas, Ca and K contents for oak filtered bio-oil were 67 and 33%, respectively. The hydroprocessed carbon fuels showed similar results for all samples regarding the oxygen content, with less than 0.6% of oxygen content in oak-based fuel and with less than 2% for switchgrass carbon fuel. Producing hydrocarbon liquid fuels by integrating HVF fast pyrolysis with catalytic hydrotreating seems to hold great potential for future applications. (Elliott et al. 2014 and Wang et al. 2016)

4.5.2 University of Twente

University of Twente in the Netherlands developed immersible filter. These filters can be integrated within a fluidised bed reactor for HVF applications (Hoekstra et al. 2009). The in-situ filtering of pyrolytic vapours avoids the extra residence time added by ex-situ filtration units, and prevents excessive secondary reactions that are responsible for the reduction of bio-oil yield. Figure 19 shows a sketch of the immersible filter positioned inside a fluidised bed. The immersible filter have a constant pressure drop, due to the continuous cleaning of its outer surface by fluidised bed materials. Series of experiments were conducted by Twente University in laboratory and bench (pilot plant; 0.7 kg/h) scale. The laboratory scale fluidised bed tests resulted in producing solid-free filtered bio-oil with no Na and Mg. However, small amounts of K were detected in the final product. Continuous pilot plant experiments investigated the influence of cake formation on pressure drop across the filter. Figure 20 shows the pressure drop profile generated during continuous pilot plant runs. Constant pressure drop across the filter was achieved after 10 minutes for 2 h long test run. Furthermore, the conducted ageing test of the filtered bio-oil was for 24 h storage at 80 °C. The ageing rate of filtered bio-oils was enhanced. However, the ageing reactions continued at lower rates, influenced by the highly reactive compounds in bio-oil, despite the lack of solid particles in the end product. (Hoekstra et al. 2009)

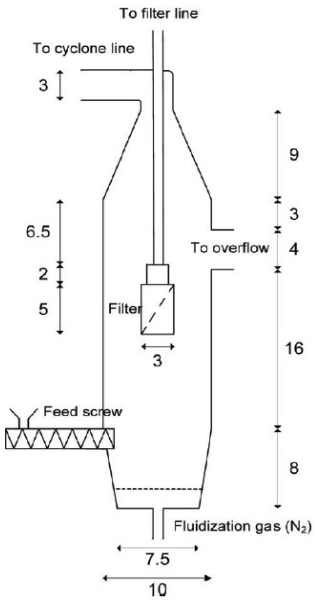

Figure 19: Dimensional sketch of the immersible filter inside a bench scale fluidised bed (Hoekstra et al. 2009).

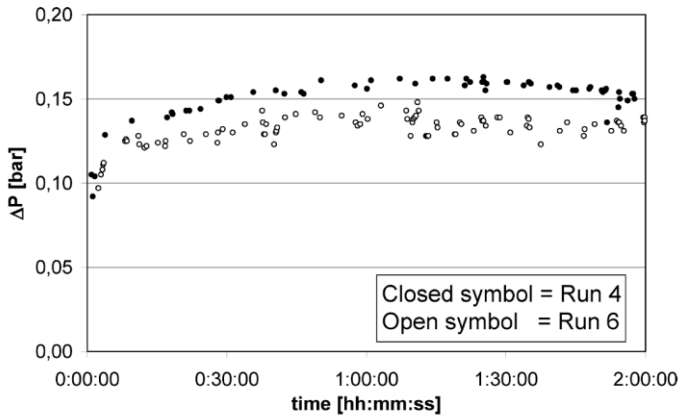

Figure 20: Pressure drop inside immersible filter during bench scale continuous pilot plant experimental runs (Hoekstra et al. 2009).

4.5.3 Technical Research Centre of Finland (VTT)

VTT began developing hot vapour filtration technique to upgrade FPBO quality and replace light and heavy fuels used in power plants and boilers (Solantausta et al. 2001). Experiments were conducted primarily with a bench-scale capacity of 1.5 kg/h. Results showed reduction in solids content below 0.1 wt. % and noticeable increase in water content. The used bench-scale filter had a filtration capacity of 50-80 l/min. Successful initial continuous runs were accomplished and stable conditions were reached. Efficient cake regeneration was achieved after 30 h of constant pressure build up, as shown in figure 21.

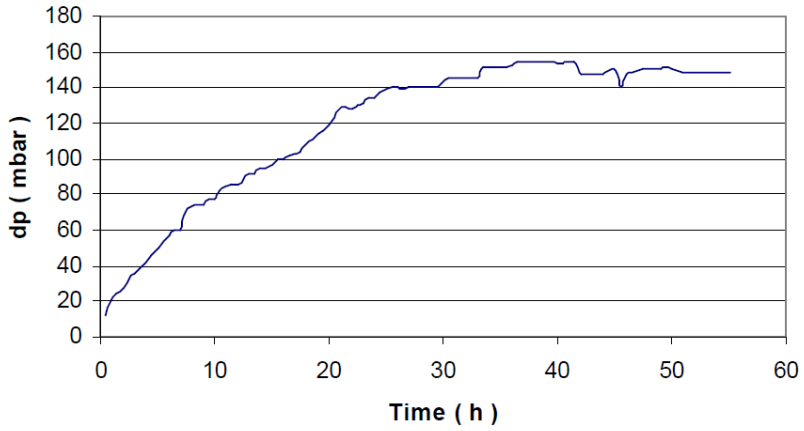

Figure 21: Pressure drop of HVF unit at bench-scale (Solantausta et al. 2001).

More experiments were conducted with the process development unit (PDU). PDU has a processing capacity of 20 kg/h. The data obtained from bench-scale experiments were used to design a larger filter for PDU with a filtration capacity of 150-500 l/min. The filter was integrated into PDU slipstream alongside a condensation unit. One meter long ceramic candles were used as filtering elements. They were commercially manufactured by USF Schumacher. Forest residues were pyrolyzed and various vapour flow rates were tested. At 100% flow rate (450 l/min), experiments resulted in efficient solid removal but inadequate cake removal. Ineffective cake removal caused persistent increase in pressure drop. At 30-40% flow rate (150 l/min), regeneration of cake by reverse pulsing was effective. Pressure-drop profile is shown in figure 22. As a conclusion, face velocity and particulate loading are very influential parameters over the formation of the cake. VTT also conducted experiments regarding the suitability of filtered bio-oil in fuel market as light or heavy fuel. Testing crude and filtered bio-oil in diesel engines, resulted in lower ignition delays and higher burning rate for the upgraded bio-oil. (Solantausta et al. 2001)

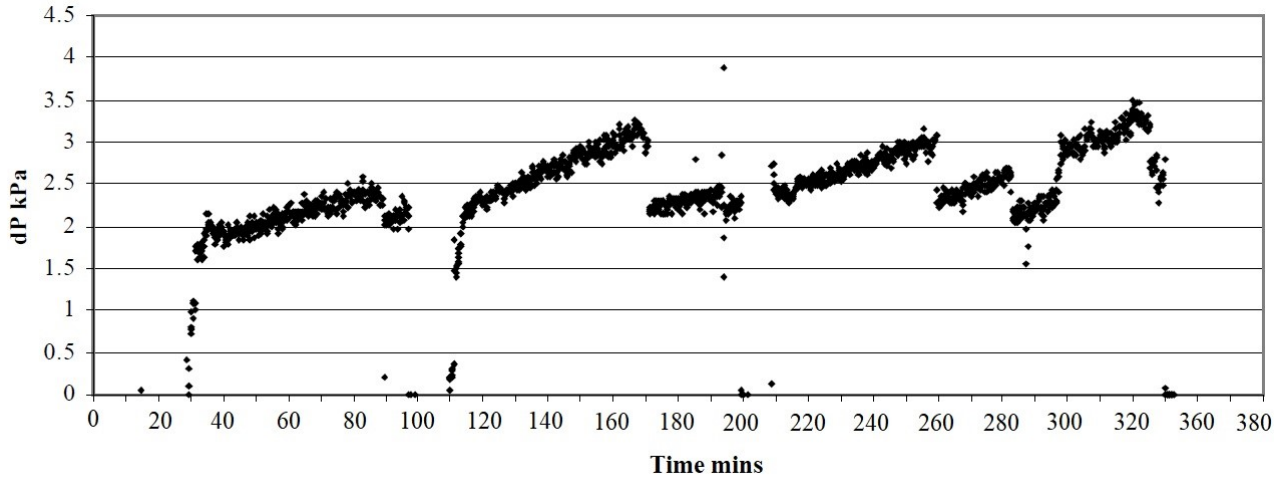

Figure 22: Pressure drop profile during 150 l/min run (Modified figure form Solantausta et al. 2001).

4.5.4 Mahasarakham University

Effect of HVF on bio-oil yield was studied by Mahasarakham University in Thailand. Initial experiments included pyrolysing agricultural residues of cassava rhizome (CR) and cassava stalk (CS) in a fluidised-bed (Pattiya and Suttibak, 2012 a). Optimum pyrolysis temperatures of 472 °C and 475 °C were selected for CR and CS feedstocks, respectively. Incorporation of HVF stage resulted in

reduction of solids content from 3.9 to 0.8 wt. % for CR, and from 3.3 to 0.6 wt. % for CS. Stability index also decreased dramatically for filtered bio-oils from 27.3 to 1.8 for CR, and from 25.9 to 1.5 for CS. In addition, lower ash content was detectable in filtered bio-oil than in untreated bio-oil. However, HVF integration affected bio-oil properties negatively by reducing its lower heating values from 23 MJ/kg to 20.5 MJ/kg. HVF also reduced filtered bio-oil yield by 6-7 wt% and increased water content by 2-13 wt%. Same researchers from Mahasarakham University tested the influence of glass wool as a filtration medium (Pattiya and Suttibak, 2012 b). Feedstocks of rice straw and husk were tested with optimal pyrolysis temperatures of 405 °C and 452 °C, respectively. The experiment resulted in a yield reduction of 4-7 wt. % for filtered bio-oils. In addition to an increase in the final water content, lower heating values were also reduced for filtered bio-oils, as a consequence. However, filtered bio-oil exhibited better properties of stability, ash content and solids content than unfiltered bio-oil. These experimental results shed light on the advantages and drawbacks of such an integration. (Pattiya and Suttibak, 2012 a and b)

4.5.5 Aston University

Since filter cake in HVF applications exhibits catalytic effect on FPBOs. Sitzmann from Aston University investigated the influence of extended residence time and secondary cracking of vapours on the final product (Sitzmann, 2009). Series of experiments with four different configurations were conducted. The produced bio-oils from all these different configurations were analyzed for comparison purposes. The first standard run was carried out with a conventional fast pyrolysis configuration and achieved 54.5 wt. % of organic yield. The second experiment included an empty fixed-bed secondary reactor after a primary cyclone; to investigate the influence of residence time solely. The second run resulted in slight reduction in organic yield with 53.7 wt. %. Third run included the same secondary reactor but filled with char. Operational temperature of the secondary reactor was set to 500 °C. Material balance calculations showed that organic yield was reduced in the presence of char from 53.7 to 46.8 wt. %, and the amounts of non-condensable gases and water increased from 15.9 to 18.6 wt. % and from 10.8 to 13.2 wt. %, respectively, as a consequence. The forth experiment included a filtration unit without filter candles instead of a secondary reactor; to investigate the influence of residence time on the final product without the impact of secondary vapour cracking. Material balance calculations showed slight decrease of organic yield from 53.7 wt. % in empty secondary reactor setup to 53.3 wt. % in empty filter vessel unit. It was concluded that

molecules decomposition is not severely affected by the extended residence time, but rather by the presence of char and AAEM, which reduce organics yield significantly due to the secondary vapour cracking. (Sitzmann, 2009)

Sitzmann also investigated cake formation on different candles with different face velocities. Some of the experiments were conducted without a primary cyclone; to direct the heavy char loads toward the filtration unit. Two different face velocities were investigated without a primary cyclone. At low face velocity of 2.0 cm/s, large char particles were separated by gravity on their way to the candle surface, resulting in a denser cake formation of fine char particles (< 20 µm). At higher face velocity of 3.4 cm/s, porous cake structure was formed containing large particle sizes (> 200 µm). Figure 23 shows scanning electron microscope (SEM) images of the cake textures as a result of different face velocities. (Sitzmann, 2009)

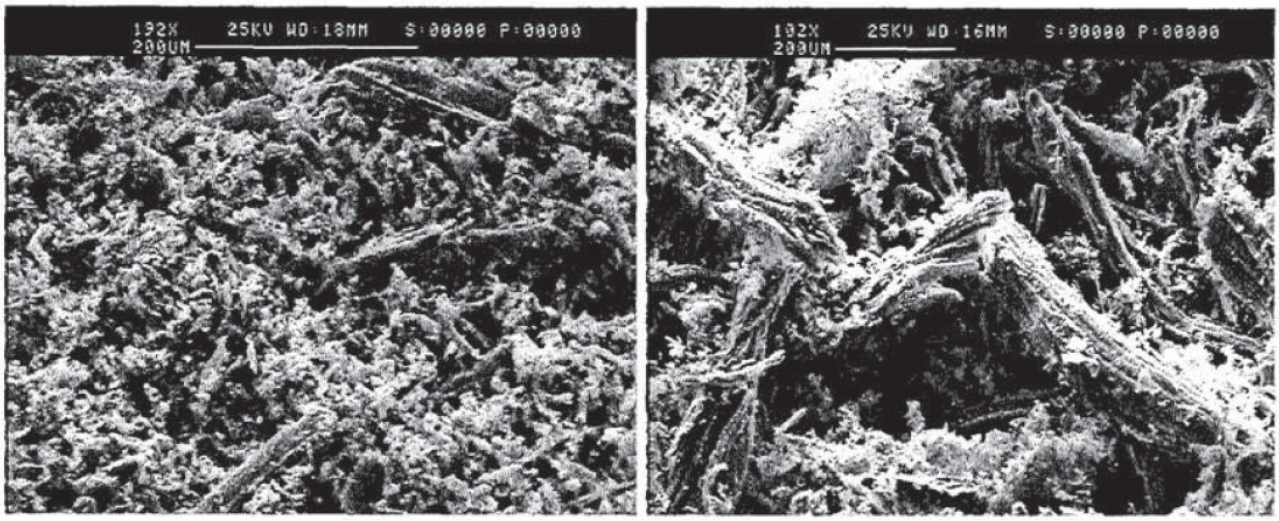

Figure 23: SEM pictures of filter cakes as a result of different face velocities; 2.0 cm/s on the left and 3.4 cm/s on the right (Sitzmann, 2009).

4.5.6 Shanghai Jiao Tong University

Shanghai Jiao Tong University conducted experiments on a 1-5 kg/h bench-scale fluidised-bed; to investigate the influence of HVF on produced FPBO (Chen et al. 2011). Rice husks were pyrolyzed. Similar pattern of results as the previously mentioned experiments was observed. Primary experiments included only a cyclone for char separation; to inspect the original yields without a filtration unit. HVF unit was later coupled with the primary cyclone to investigate the impact of

HVF. Filtered bio-oil observed a reduction in yield from 41.7 wt. % for unfiltered bio-oil to 39.5 wt. %. The secondary decomposition in HVF unit resulted in a reduction of organics and organic acids. Vapour cracking contributed significantly to higher water content and pH values for filtered bio-oil. High heating value of bio-oil increased from 22.06 MJ/kg for unfiltered bio-oil to 23.86 MJ/kg for filtered bio-oil. In addition, remarkable reduction in AAEM content was achieved for filtered bio-oil. (Chen et al. 2011)

4.6 Summary

Solids and AAEMs are some of the contaminants that contribute to the severity of ageing reactions of bio-oils during storage. Hot vapour filtration is proved to be effective in reducing solids content and in the removal of AAEMs. Reduction of contaminants is essential to protect downstream equipment and catalysts from corrosion and poisoning, respectively. Table 3 lists down the advantages and drawbacks of hot vapour filtration in a fast pyrolysis process.

Table 3: Advantages and drawbacks of hot vapour filtration.

HVF advantages	HVF drawbacks
• Reduction of AAEM content.	• Reduction of bio-oil yield.
• Reduction of solid content.	• Increase of NCG and Bio-char yield.
• Reduction of ash content.	• Cake formation (constant pressure build-up).
• Reduction of bio-oil viscosity.	• Increase of water content.
• Reduction of ageing reaction rate during storage.	• Reduction of heating values of bio-oil.
• Enhance the ability to upgrade and valorize bio-oil to different fuels by protecting downstream equipment from contaminants.	
• Better ignition (lower ignition delays and higher burning rate).	

On the other hand, hot vapour filtration have detrimental effect on bio-oil yield, by promoting further cracking of vapours due to the extended residence time across the filter. However, molecules decomposition is affected primarily by the presence of char and AAEMs rather than by the extended residence time entirely. Char and AAEMs catalytically crack vapours which results in reducing bio-oil yield. As a consequence, NCG and bio-char yields are increased. According to literature, filtered bio-oils exhibit higher water content and lower heating values, which are considered drawbacks of the upgrading process.

Furthermore, stabilizing the filtration process can be a challenging task; due to constant pressure build-up inside the filter. Pressure development is caused by cake formation over filter media. Cake formation is governed by the particulate loading and face velocity of vapours. Maintaining efficient cake regeneration is critical; to achieve a stable process and avoid pressure build-up.

Experimental part

5. Experimental runs

5.1 Introduction

The influence of hot vapour filtration (HVF) on the final product has been studied through series of runs covered in the experimental part. Different filtration temperatures have been analyzed thoroughly; to achieve a reduction in solids and Alkali and alkaline earth metals (AAEMs) contents in the final product. The utilized hot filter consists of filtration candles and moving granules, further details regarding the filter design will be later discussed.

5.2 Feedstock

Utilized raw material in conducted runs is Lassila & Tikanoja (L&T) recycled wood class B. According to the solid biofuel standard (EN ISO 17225-1) and in consonance with Alakangas et al. (2015), grade B recycled wood (used wood) contains maximum 2 wt. % of mechanical contaminants such as cement and nails. Threshold values of chlorine and heavy metal contents for grade B recycled wood are similar to virgin wood, as shown in table 4. Normative values are the essential threshold values. However, informative values such as potassium and sodium are non-mandatory and recommended for combustion behavior evaluation (Alakangas et. al. 2015).

Table 4: Class B used wood threshold values in Finland, reformed based on (Alakangas et al. 2015).

Property		Threshold value, dry basis	Virgin wood	Class B	
				Normative	Informative
Sulphur	S	≤ 0.2 wt. %	Bark, broadleaf	X	
Nitrogen	N	≤ 0.9 wt. %	Bark, broadleaf	X	
Potassium	K	≤ 5000 mg/kg	Bark, broadleaf		X
Sodium	Na	≤ 2000 mg/kg	Bark, coniferous		X
Chlorine	Cl	≤ 0.1 wt. %		X	
Heavy metals					
Σ Arsenic + Chromium+ Copper	As+ Cr+ Cu	≤ 70 mg/kg[2]	bark, coniferous Σ 74 mg/kg	X	
Cadmium	Cd	< 1 mg/kg	bark, coniferous	X	
Mercury	Hg	≤ 0.1 mg/kg	bark, coniferous	X	
Lead	Pb	≤ 50 mg/kg	bark, coniferous	X	
Zinc	Zn	≤ 200 mg/kg	bark, coniferous	X	

Utilized raw material have a particle size range of 0.5-3 mm. Table 5 presents proximate and ultimate analysis of the raw material. Recycled wood class B contains low ash content of 0.8 wt. %, and 84.7 wt. % volatile matter. Oxygen content in raw material was calculated by subtracting elemental composition of carbon, hydrogen, nitrogen and ash content from 100. Raw material analysis were done based on Finnish Standards Association (SFS).

Table 5: Proximate and ultimate analysis of recycled wood.

Proximate analysis	Unit	Value	Standard
Moisture	wt. %	8.0	SFS-EN ISO 18134-3
Volatile matter (dry)	wt. %	84.7	SFS-EN ISO 18123
Ash (dry)	wt. %	0.8	SFS-EN ISO 18122
HHV (dry)	MJ/kg	20.17	SFS-EN 18125
LHV (dry)	MJ/kg	18.86	SFS-EN 18125
Ultimate analysis			
Carbon (dry)	wt. %	50.4	SFS-EN ISO 16948
Hydrogen (dry)	wt. %	6.0	SFS-EN ISO 16948
Nitrogen (dry)	wt. %	0.4	SFS-EN ISO 16948
Oxygen* (dry)	wt. %	42.4	
Oxygen*=by difference			

AAEM content in raw material alongside other metals are presented in table 6. Calcium is abundant in recycled wood relative to other AAEM with 1700 mg/kg. Other metals quantities fall into class B threshold values mentioned previously. Analytical techniques such as inductively coupled plasma mass spectrometry (ICP-MS), inductively coupled plasma atomic emission spectrometry (ICP-AES) and oxygen bomb ion chromatography were used. Analytical techniques were conducted according to (SFS-EN ISO 16967 (A), SFS-EN ISO 17294-2, SFS-EN ISO 11885, SFS-EN ISO 16994, SFS-EN 15408, and SFS-EN ISO 10304-1).

Table 6: Alkali and alkaline earth metal content in recycled wood raw material.

	Metals	Unit	Recycled wood
AAEM	Na	mg/kg	350
	K	mg/kg	500
	Mg	mg/kg	230
	Ca	mg/kg	1700
Other metals	Cr	mg/kg	6.4
	Mn	mg/kg	80
	Fe	mg/kg	210
	Cu	mg/kg	6.4
	Zn	mg/kg	58
	Si	mg/kg	790
	Pb	mg/kg	20
	P	mg/kg	55
	S	%	0.017
	Cl	%	0.02

5.3 Experimental plan

Series of 6 runs were carried out, as it can be shown in table 7. Including 3 reference runs without HVF unit (132, 133 and 134); to optimize process temperature for the utilized raw material. It is necessary to observe the influence of HVF on organic yield. Pyrolysis temperature yielding the highest organic yield was anticipated to be in the range of 480-520 °C. Consequently three fast pyrolysis temperatures (480, 500 and 520 °C) were tested. In addition, 3 different filtration runs were carried out (135, 136 and 137), which include the HVF unit at different filtration temperatures of 450, 400 and 360 °C, respectively. Biomass feeding rate during these experiments was between 530 and 760 g/h. Nitrogen flow inside the reactor was set to 34 nl/min. However, extra 2 nl/min were added inside the filter for technical reasons which makes the total nitrogen flow inside the whole system equals to 36 nl/min for HVF runs. Duration of the experiments varied. 3 h runs were sufficient to stabilize reactor temperature during the first three runs without the hot filter. Whereas, HVF runs were 6 h long; to stabilize the temperature of the reactor and the hot filter for accurate final results.

Table 7: Experimental runs description.

General parameters	Unit	Fast pyrolysis without HVF unit			Fast pyrolysis with HVF unit		
Experimental run		132	133	134	135	136	137
Fast pyrolysis temperature	°C	500	480	520	500		
Filtration temperature	°C	No Hot Filter			450	400	360
Number of candles					3		
Nitrogen flow	nl/min	34			36		
Run time	h	3			6		

6. Experimental setup

HVF experiments were carried out with the newly designed hot filter by VTT. In the experimental setup chapter, the operational concept of the filter will be described alongside the two process configurations involved in the experimental runs.

6.1 VTT filter design

Operational concept of the hot filter is based on combining filtration candles with flowing granules. The flowing sand granules assure continuous regeneration of cake over the candles. In addition to that, moving granules function as initial filtering media for particle-laden vapours. Constant pressure difference across the filter can be achieved by integrating the two technologies in the designed filter. The design is a combination of the two technologies mentioned in chapter 4.2.1 and 4.2.2, and similar to the one tested by University of Twente, however the filtration system is not integrated within the main pyrolysis reactor.

The hot filter comprises 3 ceramic candles with a pore size of 0.3 µm. As it can be seen in figure 24, quartz sand granules are heated in a sand heater vessel before passing through the hot filter where candles are placed. The sand is drawn out of the filter during the experimental run by a screw conveyor into a collection vessel. HVF unit was designed to achieve solid content <0.1 wt. %. In addition to stable continuous regeneration of char cake.

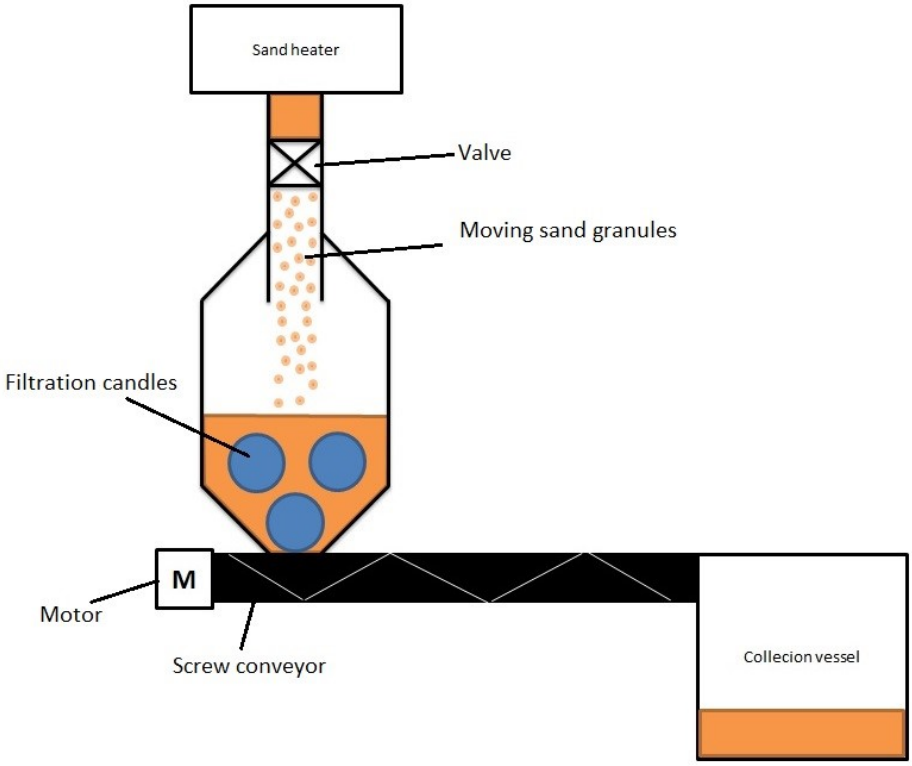

Figure 24: Hot vapour filter designed by VTT.

6.2 Process configuration

All experiments were conducted with the bench-scale unit (1 kg/h). The unit can be reconfigured by adding or removing the hot filter. The fast pyrolysis setup consists of bubbling fluidized bed, cyclones, HVF unit, condensers and electrostatic precipitator. Nitrogen gas is used to fluidize the bed as raw materials are fed into the reactor using a screw feeder. Aluminum oxide is used in the bubbling fluidised-bed reactor as a bed material. Char is collected from the first and second cyclones prior to the collection of pyrolysis liquids from the recovery train. Gas chromatograph device is attached to analyze the gas content at different runs.

Runs 132, 133 and 134 were conducted with configuration (A) setup without the hot filter as presented in figure 25. The liquid recovery section includes water condenser, electrostatic precipitator (ESP) and two glycol condensers. In the first three runs, recycled wood was pyrolysed at different temperatures (480, 500 and 520 °C); to decide the optimal pyrolysis temperature with the highest organic liquid yield.

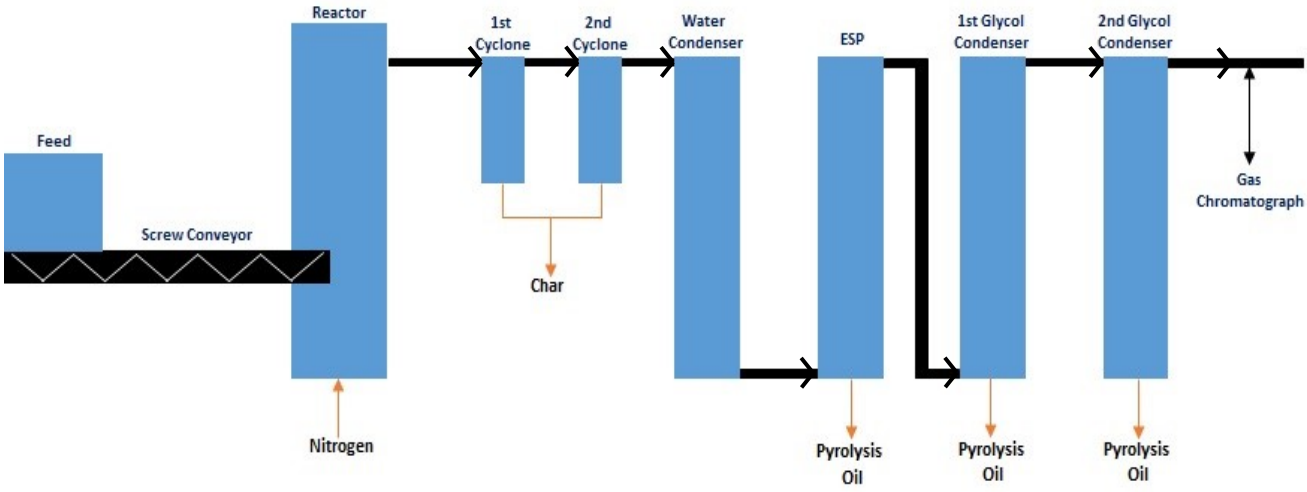

Figure 25: Configuration (A) setup without HFV unit.

Runs 135, 136 and 137 were carried out with configuration B setup that includes the hot filter, as shown in figure 26. These runs investigate the influence of HVF at different filtration temperatures. The majority of char particles are separated by cyclones followed by complete collection of fine char particles inside the filter prior to the liquid recovery stage. The liquid recovery train in configuration (B) consists of water condenser, ESP and one glycol condenser. Experiments were carried out with these two separate existing configurations. Produced bio-oils from each condensing column were mixed for every run and analyzed in the laboratory.

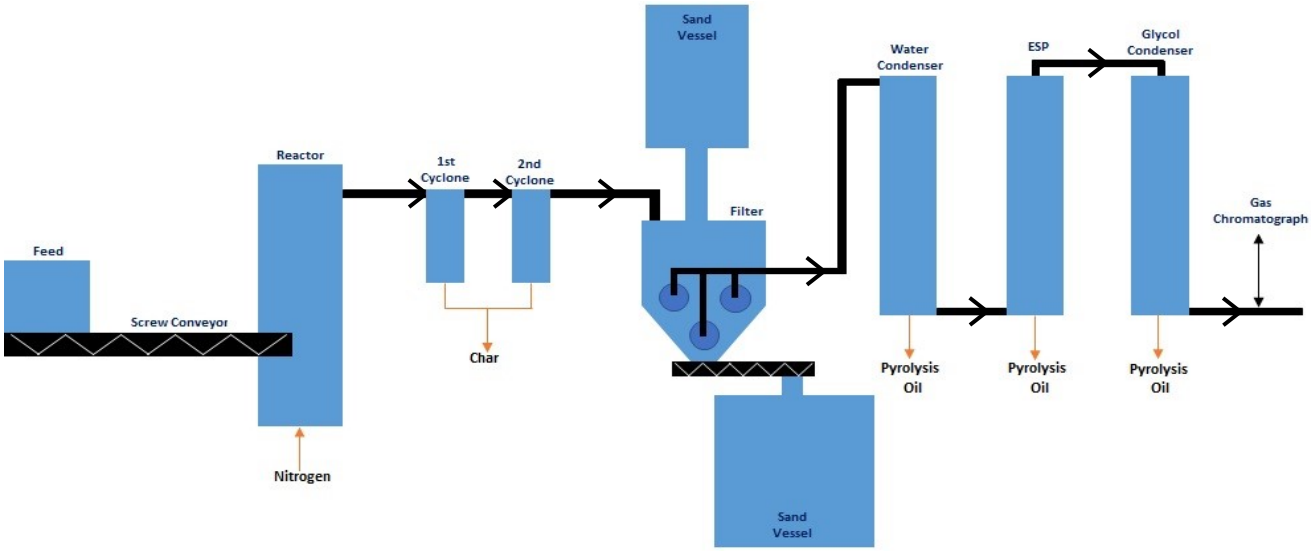

Figure 26: Configuration (B) setup with HFV unit.

7. Results and discussion

7.1 Fast pyrolysis runs without HVF

As mentioned earlier, the first three runs were carried out without the hot filter. Detailed mass balance of runs 132, 133 and 134 can be found in Appendix 1, these runs correspond to pyrolysis temperatures of 500, 480 and 520 °C, respectively. Figure 27 shows products yield at different pyrolysis temperatures. Some of the values fall within the experimental error bars of 3 %, however one experiment was conducted at each pyrolysis temperature due to time constraints. Based on material balance calculations, organic yield improved slightly from 54 to 55 wt. %, as the temperature increased from 480 to 500 °C. Further increase of temperature to 520 °C reduced organic yield to 52 wt. %. On the other hand, pyrolytic gas yield increased as pyrolysis temperature changed from 480 to 520 °C. Whereas, cyclone char and pyrolytic water yields were consistent despite the temperature change.

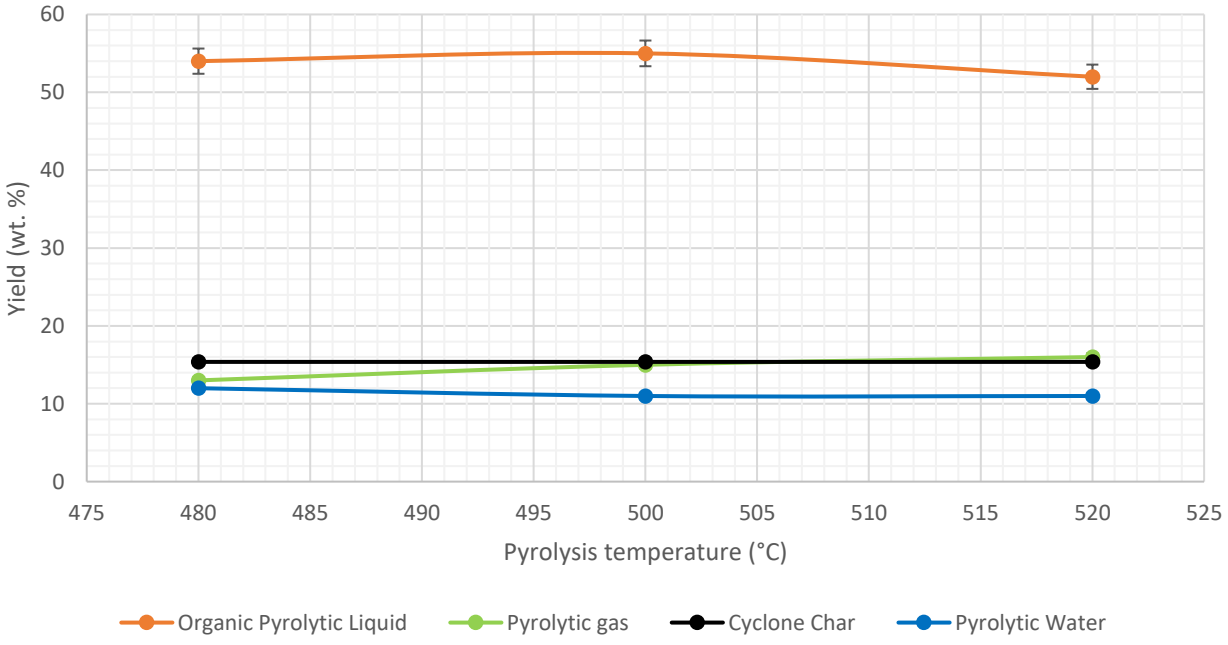

Figure 27: Products yields at different temperatures (480, 500 and 520 °C).

Table 8 presents the physiochemical properties of produced bio-oils from the first three runs. All bio-oil analysis were done at VTT laboratories. Wet samples were analyzed, however the elemental composition alongside other properties were calculated to a dry basis; by subtracting the hydrogen content found in water and by excluding water content in the dry basis calculations of carbon,

nitrogen and other properties. Oxygen is calculated by the difference of elemental composition on a dry basis. Elemental analysis of bio-oil and its fractions was done using Elementar Vario Max CHN analyzer following (ASTM D 5291). Bio-oil elemental composition is necessary to evaluate its quality by calculating H/C and O/C ratios. Compared to light petroleum products with H/C ratio of 1.5-1.9 (Ates et al. 2005), bio-oil from runs 132, 133 and 134 had H/C ratio of 1.40, 1.29 and 1.39, respectively. The calculated O/C ratios were expected to be in the range of 0.5 as the utilized raw material is rich in oxygen.

Table 8: Physiochemical properties of produced bio-oils from runs 132, 133 and 134.

Property	Unit	Run		
Experimental run		132	133	134
Pyrolysis temperature	°C	500	480	520
Water	wt. %	16.3	19.4	18.4
Solids	wt. %	0.20	0.20	0.20
Ash	wt. %	< 0.05	< 0.05	< 0.05
MCR (dry)	wt. %	28.1	28.4	28.7
TAN (dry)	mg KOH/g	63.7	73.5	63.6
Carbonyl (dry)	mmol/g	5.34	5.33	5.27
WIS (dry)	wt. %	33.2	43.9	32.0
HHV (as produced)	MJ/kg	19.3	18.8	19.0
HHV (dry)	MJ/kg	23.1	23.4	23.3
LHV (as produced)	MJ/kg	17.7	17.3	17.4
LHV (dry)	MJ/kg	21.6	22.1	21.8
H/C (dry)	molar ratio	1.40	1.28	1.39
O/C (dry)	molar ratio	0.499	0.503	0.491
Elemental composition (wt. %)				
Carbon (dry)	wt. %	55.7	55.8	56.1
Hydrogen (dry)	wt. %	6.54	5.99	6.55
Nitrogen (dry)	wt. %	0.72	0.74	0.61
Oxygen* (dry)	wt. %	37.0	37.4	36.7
Oxygen *: by difference				

Water content analysis of bio-oil has been done by Karl Fischer titration using Metrohm 795 KFT Titrino titrator according to (ASTM E 203). The lowest water content of 16.3 wt. % has been achieved at a pyrolysis temperature of 500 °C. Bio-oils produced during run 133 and 134 contained high water contents of 19.4 and 18.4 wt. %, respectively. Solids content of bio-oils were determined by filtration of solids in methanol according to (ASTM D 7579). Solid contents remained the same at different pyrolysis temperatures with 0.20 wt. %.

Analyzing micro carbon residue (MCR) of bio-oil is beneficial to evaluate the effectiveness of HVF within the process. MCR reveals the tendency of bio-oil to form coke, which is vital for further upgrading of pyrolytic oil. MCR analysis was done according to (ASTM D 4530) using Alcor Micro Carbon Residue Tester. MCR dry basis results showed consistency at different pyrolysis temperatures, ranging between 28.1-28.7 wt. %, as shown in table 8. MCR samples were later used to determine the ash content of bio-oils by burning them in a muffle oven at 775 °C. Produced bio-oils contained low ash content below 0.05 wt. %. Total acid number (TAN) was measured using 785 DMP Titrino analyzer following (ASTM D 664). Bio-oil produced in run 132 and 134 were slightly less acidic compared to the one produced at 480 °C during run 133. High acidity is due to the presence of volatile acids and other compounds, such as phenolics, hydroxy acids, fatty and resin acids (Oasmaa et al. 2010). Phenolic Carbonyl compounds were analyzed to investigate the stability of bio-oils during storage. According to Diebold (2002) and Oasmaa et al. (2003), carbonyl species contributes to the instability of bio-oils during storage. Reduction of carbonyl compounds correlates with the severity of ageing reactions during storage (Oasmaa et al. 2011). One year storage conditions will be mimicked while observing the changes in carbonyl compounds in bio-oils. Similar to viscosity increase-based stability test, carbonyl titration method will show correlative stability results and examine the severity of ageing reactions during storage (Oasmaa et al. 2011).

Water insoluble (WIS) fraction was analyzed by mixing 5 ml of oil sample and 35 ml of water. The mixture was then filtered through a semi permeable filter paper. Bio-oil produced from these runs had WIS contents ranging between 32 and 43.9 wt. %. Higher and lower heating values (HHV and LHV) were determined by using IKA Werke C 5000 control calorimeter according to (DIN 51900). HHV ranged between 23.1-23.4 MJ/kg, whereas, LHV of produced bio-oils ranged between 21.6-22.1 MJ/kg. Based on these observations, 500 °C was selected as pyrolysis temperature for hot vapour filtration runs with the hot filter, as it yields the highest organic liquids with the lowest water content.

7.2 Fast pyrolysis runs with HVF

Hot vapour filtration experiments were subsequently commenced after deciding the optimum pyrolysis temperature for recycled wood. Filtration runs conditions were selected based on various filtration temperatures.

The filtration temperatures selected for runs 135, 136 and 137 were 450, 400 and 360 °C, respectively, as shown in table 9. All these runs were carried out with three filtration candles inside the hot filter with a calculated face velocity of 1.1-1.2 cm/s.

Table 9: Hot vapour filtration experiments.

HVF Parameters	Unit	Run		
Experimental run		135	136	137
Pyrolysis temperature	°C	500	500	500
Filter temperature	°C	450	400	360
Number of candles		3	3	3
Face velocity	cm/s	1.1-1.2		
Particle size of sand	mm	0.1-0.6		
Sand flow	kg/h	3		

Detailed mass balance of these runs can be found in Appendix 2. As revealed in figure 28, bio-oil yields declined from 59 to 51 wt. % just as filtration temperature increased from 360 to 450 °C, while the average cyclone char yield remained roughly the same during these runs; ranging from 14 to 15 wt. %. Elemental analysis was done on filter sand to measure char deposition during filtration runs. As shown in figure 28, filter char yield range is between 2 and 3 wt. % across all filtration temperatures.

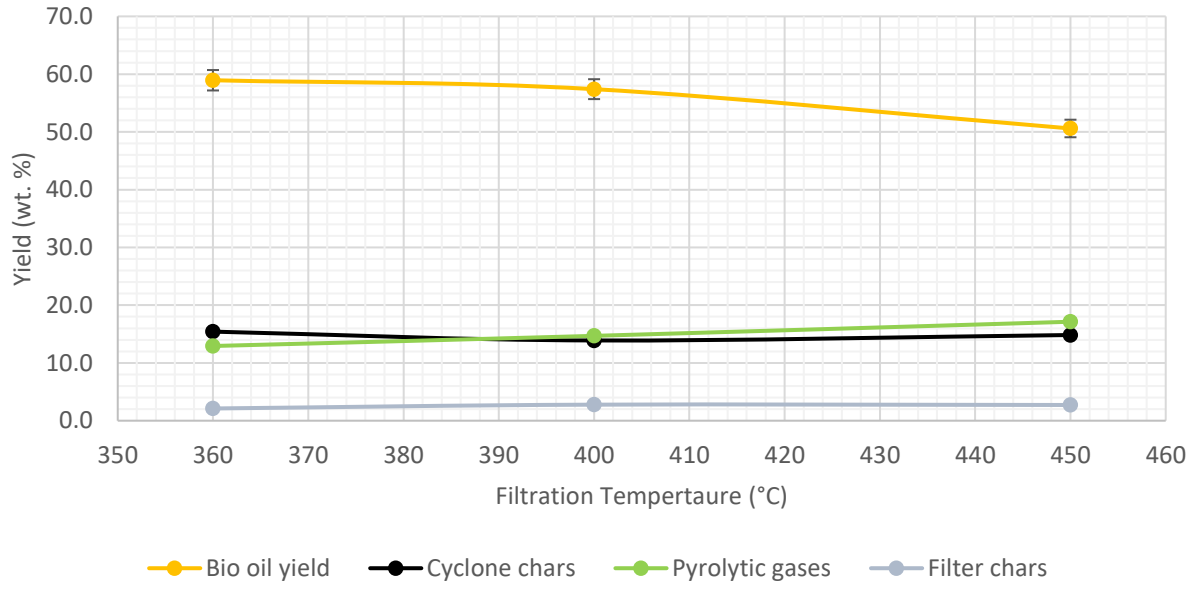

Figure 28: Pyrolytic products yields at different filtration temperatures in run 135, 136 and 137.

On the other hand, pyrolytic gas yields displayed consistent increase from 13 to 17 wt. %, as the filtration temperature increased from 360 to 450 °C. The reduction in bio-oil yields and the increase in gas yields were attributed to secondary cracking of vapours at high filtration temperatures.

Figure 29 presents the organic and water fractions of bio-oils at different filtration temperatures. As it can be noticed, secondary cracking of vapours resulted in the reduction of organic fractions, as the filtration temperature increased above 360 °C. Whereas, pyrolytic water fractions remained roughly the same at 11 wt. % during all filtration runs. However filtered bio-oil exhibited higher water content than the unfiltered one. As shown in table 10, water contents during run 135, 136 and 137 were 22.4, 21.2 and 22.6 wt. %, respectively. While the unfiltered bio-oil from run 132 had a water content of 16.3 wt. %. The increase in water content is attributed to larger quantities of moistened raw materials being processed during 6 h filtration runs compared to 3 h normal fast pyrolysis runs, in addition to different liquid recovery system in configuration (A) and (B).

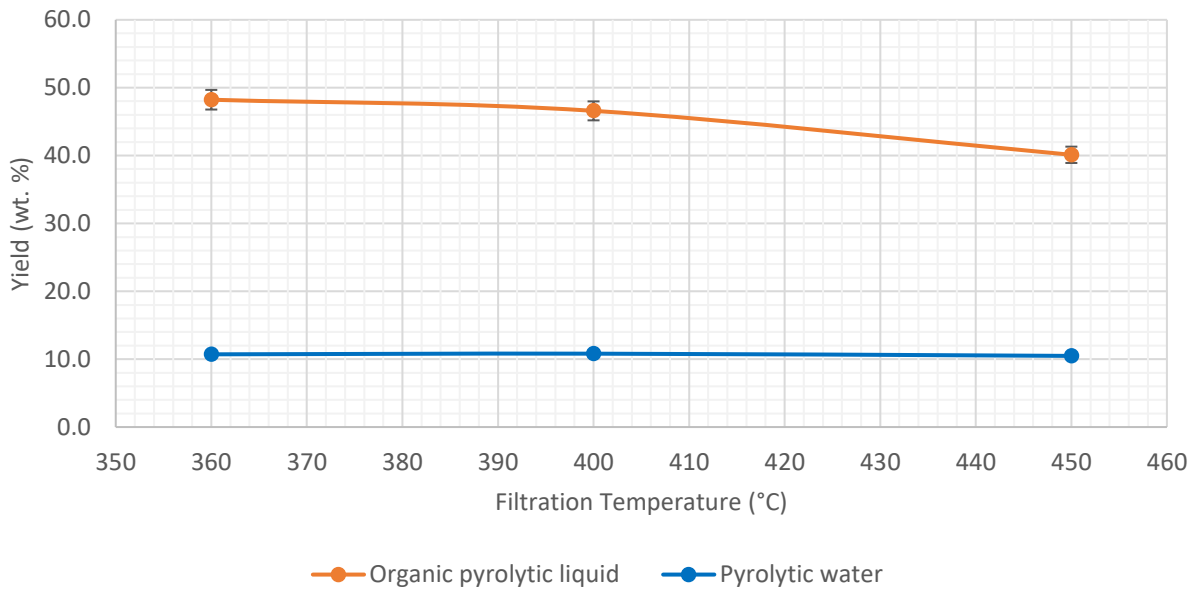

Figure 29: Organic and water fractions of the produced bio-oil from runs 135, 136 and 137.

Solids content reduced from 0.2 wt. % for unfiltered bio-oil to 0.1 wt. % for the filtered ones. The lowest solids content was achieved at a filtration temperature of 360 °C; less than 0.1 wt% of solids have been detected. As a consequence, the tendency to form coke has been reduced for filtered bio-oils. Some of MCR values are within the measurement error of the device. However, the lowest

MCR value of 24.5 wt. % was attained at a filtration temperature of 360 °C during run 137. Presence of ash in filtered bio-oils remained significantly low; below 0.05 wt. %.

Table 10: Physiochemical properties comparison between unfiltered bio-oil (run 132) and filtered bio-oils from runs 135, 136 and 137.

Products	Unit	Run			
Experiment run		132 (Unfiltered)	135 (filtered 450 °C)	136 (Filtered 400 °C)	137 (Filtered 360 °C)
Water	wt. %	16.3	22.4	21.2	22.6
Solids	wt. %	0.2	0.1	0.1	< 0.1
Ash	wt. %	< 0.05	< 0.05	< 0.05	< 0.05
MCR (dry)	wt. %	28.1	27.8	27.7	24.5
TAN (dry)	mg KOH/g	63.7	83.2	76.3	75.5
Carbonyl (dry)	mmol/g	5.34	5.15	4.95	5.04
WIS (dry)	wt. %	33.2	38.9	31.6	38.5
HHV (as produced)	MJ/kg	19.3	18.7	18.7	18.1
HHV (dry)	MJ/kg	23.1	24.1	23.7	23.4
LHV (as produced)	MJ/kg	17.7	17.0	17.1	16.5
LHV (dry)	MJ/kg	21.6	22.6	22.4	22.1
H/C (dry)		1.40	1.44	1.34	1.31
O/C (dry)		0.499	0.455	0.481	0.499
Elemental composition (wt. %)					
Carbon (dry)	wt. %	55.7	57.5	56.7	55.9
Hydrogen (dry)	wt. %	6.54	7.0	6.4	6.2
Nitrogen (dry)	wt. %	0.72	0.6	0.5	0.6
Oxygen[a] (dry)	wt. %	37.0	34.9	36.3	37.2
[a] : By difference					

Hot vapour filtration had a negative impact on bio-oils heating values (as produced basis), as shown in table 10. The reduction in heating values could be associated to the high water content in filtered bio-oils. Additionally, filtered bio-oils exhibited slight change in its elemental composition. Oxygen content dropped from 37.01 wt. % for unfiltered bio-oil to 34.9 and 36.3 wt. % for filtered bio-oils at 450 and 400 °C. However, oxygen content increased to 37.2 wt. % for filtered bio-oils at 360 °C. Nevertheless, oxygen carbon ratio remained the same at 0.499.

As observed from the TAN values in table 10, hot vapour filtration contributes to the production of organic acids. However, filtered bio-oil at 360 °C achieved the lowest increase in total acid number with 75.5 mg KOH/g compared to 63.68 mg KOH/g for unfiltered bio-oil.

One year storage conditions was mimicked by heating up the samples to 80 °C for 24 h. Carbonyl decrease-based stability test was performed and carbonyl contents were measured for all samples. As shown in figure 30, Initial carbonyl contents dropped 41.8 % for unfiltered bio-oil and 35.5 % for both filtered bio-oils at 400 and 360 °C. Ageing reaction rate was reduced at those filtration temperatures. However, at 450 °C, carbonyl content dropped 42.5 wt. %; making the ageing reaction rate similar to the unfiltered bio-oil.

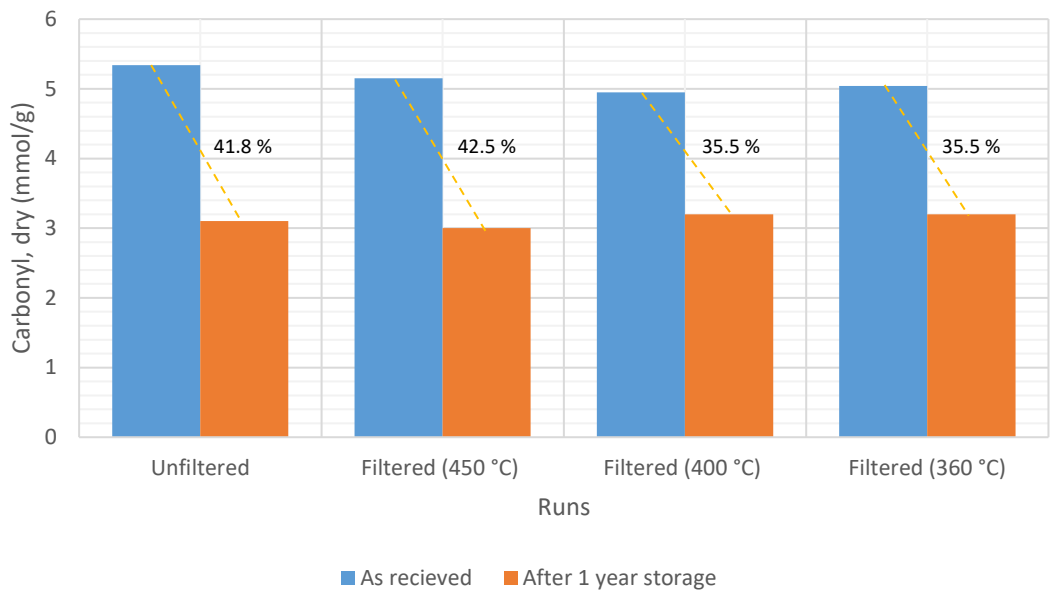

Figure 30: Carbonyl content (dry) for unfiltered and filtered bio-oils; percentage indicates carbonyl decrease due to the severity of ageing reactions.

Alkali and alkaline earth metals alongside some other heavy metals have been analyzed for unfiltered and filtered bio-oil. Table 11 lists down the analysis results. Bio-oil metal analysis techniques were similar to the previously mentioned techniques in chapter 5.2. Potassium and magnesium quantities were less than 10 mg/kg for unfiltered and filtered bio-oils. However, sodium contents were reduced 9.5 and 4.8 % for filtered bio-oil at 450 and 400 °C, respectively. Remarkable reduction of 16.7 % in sodium content was achieved at 360 °C. Initial calcium contents were reduced

from 28 mg/kg to less than 10 mg/kg for all filtered bio-oils. General reduction trends for heavy metals can be noted for filtered bio-oils. Hot vapour filtration proved to be effective in enhancing bio-oil stability during storage by reducing AAEM and heavy metal contents.

Table 11: Metal analysis of unfiltered and filtered bio-oil.

		Unit	Unfiltered	Filtered (450 °C)	Filtered (400 °C)	Filtered (360 °C)
AAEM	Na	mg/kg	84	76	80	70
	K	mg/kg	<10	<10	<10	<10
	Mg	mg/kg	<10	<10	<10	<10
	Ca	mg/kg	28	<10	<10	<10
Other metals	Cr	mg/kg	<0.5	<0.5	0.74	0.66
	Mn	mg/kg	<1	<1	<1	<1
	Fe	mg/kg	18	3.9	<1	2.4
	Cu	mg/kg	<0.5	<0.5	<0.5	<0.5
	Zn	mg/kg	1.8	0.98	0.83	0.98
	Si	mg/kg	51	85	19	14
	Pb	mg/kg	<0.5	<0.5	<0.5	<0.5
	P	mg/kg	<10	<10	<10	<10
	S	%	0.018	0.013	0.006	0.011
	Cl	%	0.026	0.034	0.02	0.019

Pressure profiles of the hot filter manifest clearly the regeneration efficiency of char cake over filtration candles. Consistent pressure build up during the 6 h run is an indication of inefficient regeneration of char cake. Figure 31 (a), (b) and (c) illustrate the outlet, inlet and differential pressure profiles of the hot filter during run 135, 136 and 137. These runs correspond to different filtration temperatures of 450 °C, 400 °C and 360 °C, respectively. Filtration temperature is a crucial parameter in regards to filtration stability and efficiency.

As indicated in figure 31 (a), pressure build-up was noticeable during run 135 at 450 °C. As filtration temperature decreases to 400 °C, filtration efficiency improves slightly. Nevertheless, differential pressure across the filter during run 136 was modest. Best regeneration of filter cake was achieved during run 137 at 360 °C. Differential pressure across the filter was stable during the run, as it can be seen in figure 31 (c).

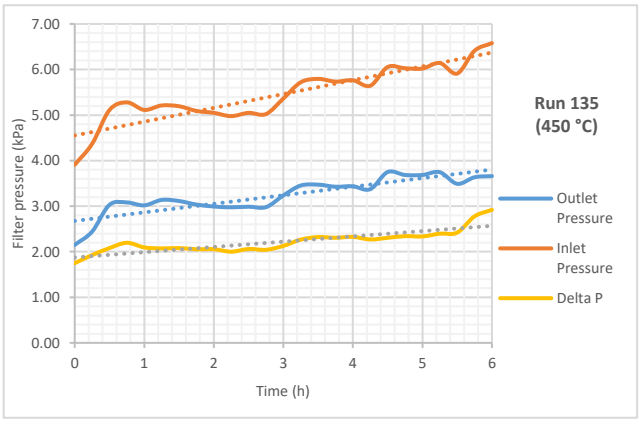

(a)

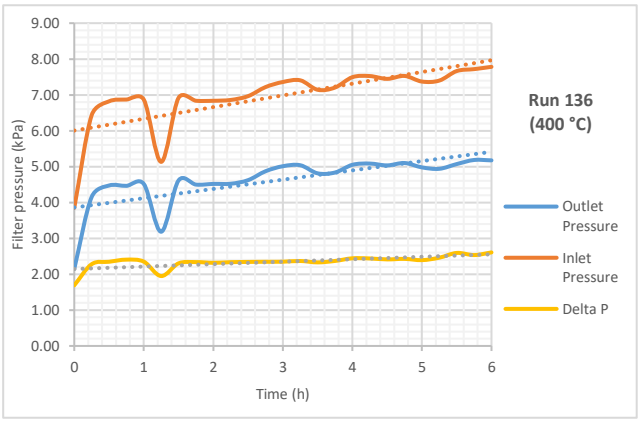

(b)

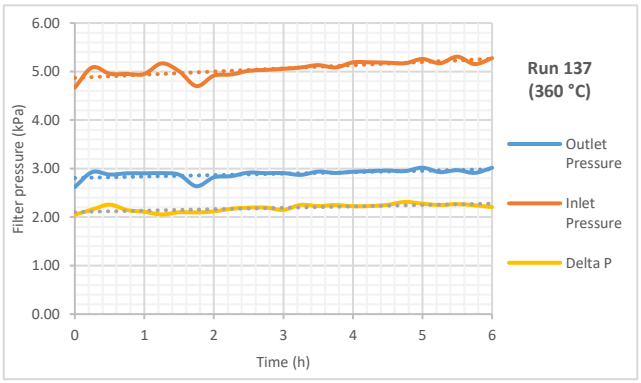

(C)

Figure 31: Inlet, outlet and differential pressures of the hot filter during (a) run 135 at 450 °C, (b) run 136 at 400 °C and (c) run 137 at 360 °C.

7.3 Discussion

Hot vapour filtration at 360 °C appears to be the most stable filtration temperature. Efficient regeneration of cake was achieved at 360 °C with constant differential pressure across the hot filter. In addition to that, minimal solids content of less than 0.1 wt. % was obtained at the same filtration temperature. Fine char particles and AAEMs were reduced significantly for filtered bio-oils at all filtration temperatures. Significant reduction of sodium was attained at 360 °C. Ageing reaction during storage did not stop completely. However, ageing reaction rate was improved for filter bio-oils at 400 and 360 °C. Table 12 presents detailed mass balance comparison between unfiltered and filtered bio-oil at 360 °C; highlighting the filtration influence on various products yields. Organic yield observed a reduction of 6.5 wt. % for filtered bio-oil. Reaction water yield observed a minor reduction of 0.04 wt. % as well. On the other hand, char featured the highest increase in yield with 2.72 wt. %; combining filter and cyclone chars. Gas yield increased for all the other filtration temperatures. However, a minimal increase of 0.08 wt. % was calculated at 360 °C.

Table 12: Detailed mass balance comparison between unfiltered bio-oil and filtered one at 360 C.

Yields	Unit	Unfiltered bio-oil (RUN 132)	Filtered bio-oil (RUN 137)	Filtration effect	Trends
Organic	wt. %	54.73	48.23	- 6.50	Organic yield reduction.
Char	wt. %	14.82	17.54	2.72	Char yield increase.
Gas	wt. %	12.85	12.93	0.08	Gas yield increase.
Reaction water	wt. %	10.75	10.72	- 0.04	Water yield reduction

8. Scalability

Scaling up the hot filter is a necessary step to evaluate its feasibility at a larger scale. Pilot-scale filter would have its own challenges that might obstruct its commercialization. At a pilot-scale process, pyrolytic vapours are dirtier than the one produced in a bench-scale. Moreover, material constraints need to be tested under heavier loads, while maintaining continuous regeneration of char cake over the surface of the candle. These are some of the key issues that need to be examined at a pilot-scale.

8.1 Preliminary design

The initial design is based on achieving face velocity of 2.03 cm/s at an operational fluidization velocity. The design face velocity was calculated based on bench-scale processed vapours and filtration surface area. 6 cm in diameter and 100 cm long candles were selected to design the pilot-scale filter. Multiple fluidization velocities were considered to attain the required face velocity. Detailed calculations regarding various design parameters can be found in Appendix 3.

Achieving the design face velocity requires balancing between fluidization velocity and surface area. Table 13 lists some of the design parameters that are used to scale up the hot filter. Water, organics and gases flow rates are 86, 23 and 63 l/min, respectively. 561 nl/min of fluidization gas is needed to attain fluidization velocity of 8 m/s. The flow of gases at 500 °C is equal to 2077 l/min. Consequently, the minimum required surface area to achieve the design face velocity is equal to 1.71 m^2, which is equivalent to the surface area of 9 filtration candles.

Table 13: Pilot-scale design parameters.

Pilot-scale reactor design parameters	Unit	Values
Utilized fluidization velocity	m/s	8
Fluidization gas required	nl/min	561
Water	l/min	86
Organics	l/min	23
Gases	l/min	63
SUM	l/min	733
SUM at 500 °C	l/min	2077
Pilot-scale filter design parameters		
Design face velocity in filter	cm/s	2.03
Min. required surface area	m^2	1.71
Surface area of 9 candles	m^2	1.70
Face velocity over 9 candles	cm/s	2.04

Figure 32 shows cross sectional area and schematic figure of the pilot filter. Filter vessel is placed over a screw conveyor that is intended to draw the sand out of the filter at a controlled rate. Pyrolytic gases flow into the filter from the top and through filter candles. Detailed calculations concerning filter dimensions and capacity can be found in Appendix 4 and 5.

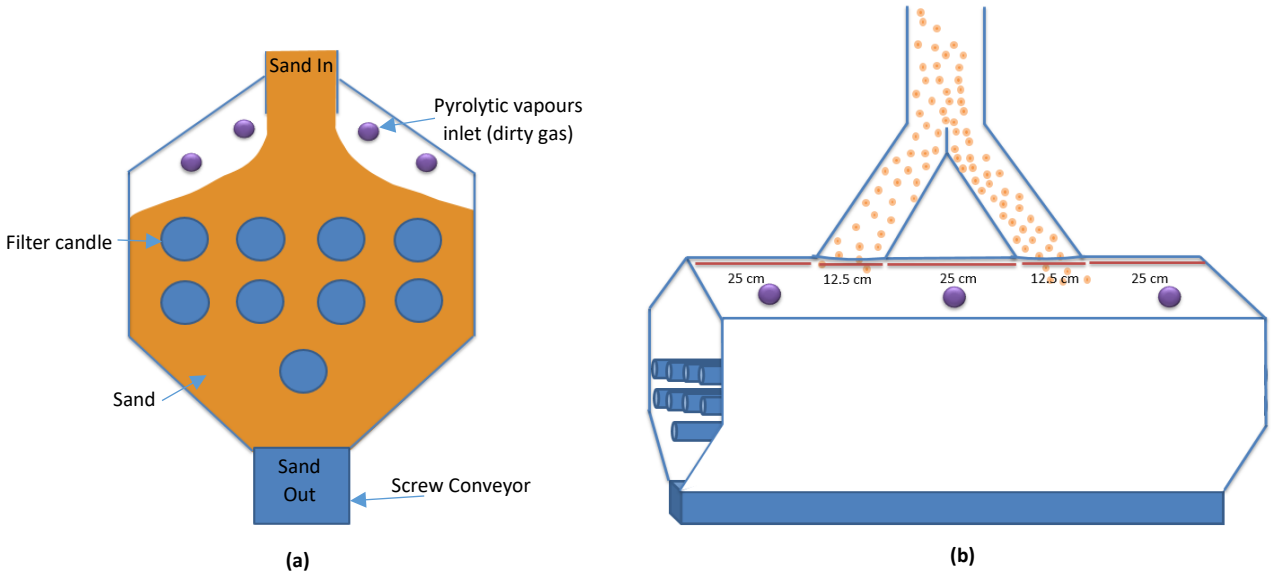

Figure 32: Pilot-scale filter (a) cross sectional area (b) 3d schematic figure.

Table 14 lists some of the general design specifications, such as pilot filter dimensions and volume. At pilot-scale filter, the recommended sand flows range between 9.7 and 19.4 l/h which correspond to 14-28 kg/h.

Table 14: Filter general design specifications.

Pilot filter parameters	Unit	Values
Total vessel volume	L	202.5
Sand volume	L	110.2
Total candles volume	L	25.70
Filter vessel height	cm	86
Filter vessel width	cm	44
Filter vessel length	cm	101
Filter vessel weight	kg	58.5
Sand flow (pilot-scale)	l/h	9.7 - 19.4

8.2 Pilot-scale integration

The 9 candles filter can be integrated within a pilot system right after the cyclone. In this case, the pilot-scale reactor is a circulating fluidized bed. Accumulated sand inside the cyclone is usually sent straight to the burner (sand heater) to be inserted back into the reactor after completing full cycle. Instead of relying on a separate source of sand to regenerate filter candles, some of the circulating sand can be employed to regenerate filtration candles. As shown in figure 33, sand fills the first cyclone and overflows to the buffer tank. The sand can be conveyed up to the top of the filter vessel, by a tilted conveyor. As the upper level indicator mounted on the cyclone flashes, the operator can open the valve for few seconds to empty the sand from the cyclone. During the refilling of sand, the buffer tank acts as a secondary storage vessel; to draw sand from for filtration purposes. The sand cycle across the filter is the longest during operation, which assures a filled buffer tank for a continuous fast pyrolysis process.

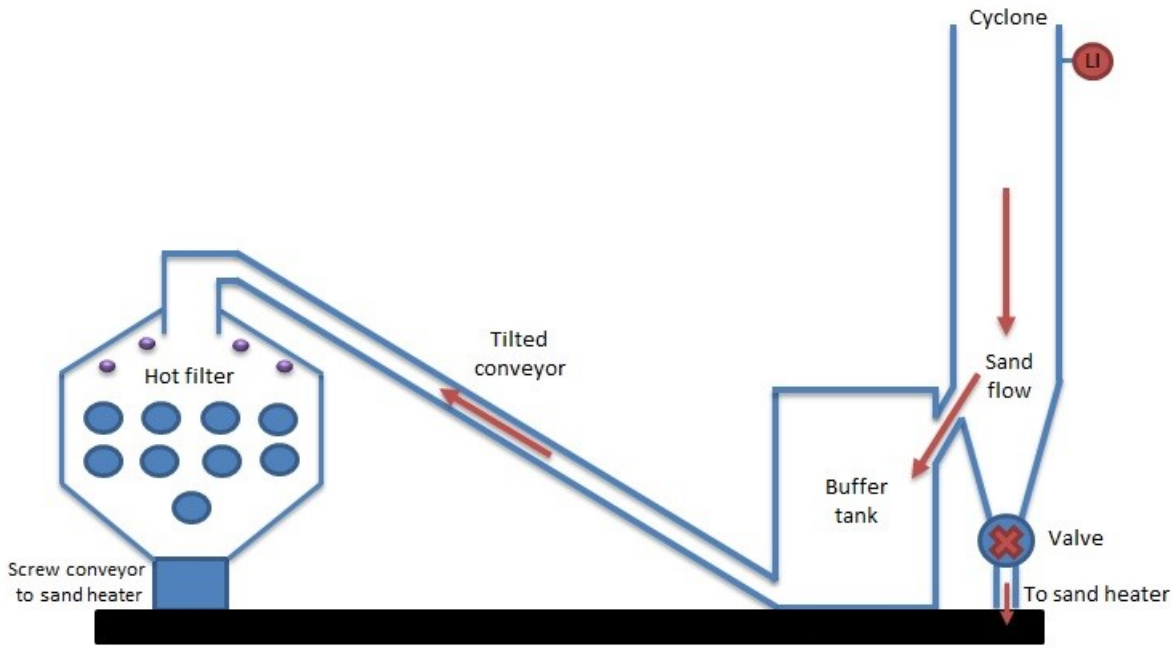

Figure 33: Integration of hot filter at pilot-scale.

During operation, filtration sand is directed back to the sand heater to complete a full cycle. Uniform unloading of sand is necessary; to maintain effective regeneration of candles and constant differential pressure across the hot filter. Uniform unloading of granules can be achieved by employing either one of following auger configurations, uniform pitch auger with decreasing inner diameter or uniform inner diameter auger with increasing pitch towards the outlet, as shown in figure 34 (Jones and Kocher, 1995).

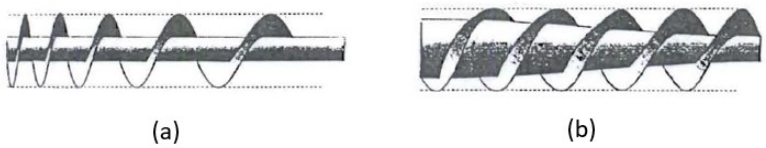

Figure 34: Two auger configurations for uniform unloading (a) increasing pitch auger, and (b) decreasing inner diameter auger (Jones and Kocher, 1995).

9. Conclusions and recommendations

Recycled wood was pyrolysed using bench-scale bubbling fluidised-bed and hot vapour filtration unit at various pyrolysis and filtration temperatures. Mass balance calculations revealed that 500 °C is the optimal pyrolysis temperature for recycled wood, which gave maximum organic yield of 55 wt. % without including the hot filter. Incorporation of hot vapour filter led to the reduction of organic yield; due to the extended residence time inside the hot filter and the catalytic effect of char and AAEMs. The minimum reduction in yield was achieved at a filtration temperature of 360 °C, with 6.5 wt. % decrease in organic yield. Consequently, hot vapour filtration influenced gases and char yields. Pyrolytic gases increased from 13 to 17 wt. % just as filtration temperature raised from 360 to 450 °C, while char yields increased significantly during filtration.

Removal of AAEMs and reduction of solids below 0.1 wt. % were achieved simultaneously at 360 °C. Filtration at 360 °C was stable during the 6 h run due to efficient regeneration of cake over filtration candles. Combining moving granules with ceramic candles assures efficient and continuous filtration process at bench-scale.

Mid-run filtration of pyrolytic vapours is an effective way to improve stability of bio-oil during storage. Alkali and alkaline earth metals were reduced significantly for filtered bio-oils. Maximum reduction of 16.7 % was achieved for sodium at 360 °C. Carbonyl-decrease stability test was carried out to measure the severity of ageing reaction during storage. The test revealed that ageing reaction rate was reduced during storage for filtered bio-oils with low solids and AAEMs contents. However, ageing reaction did not stop entirely, due to the presence of highly reactive compounds.

Hot filter was scaled up based on a design face velocity of 2.03 cm/s. The value was calculated based on vapour flow rate and filtration candles surface area at bench-scale. Preliminary design of 9-candles filter was introduced at the end of the study. Several experiments can be carried out to optimize the preliminary design of the pilot filter. Future work might include testing the influence of residence time inside the filter; different runs can be carried out with various face velocities at a filtration temperature of 360 °C. This can be achieved by substituting one of the filtration candles with an impermeable cylinder that reduces the volume inside the filter and decreases the surface area of filtration candles. In addition to that, different configurations of candles can be tried out to

enhance pressure gradient across the filter. More experiments of that sort are necessary to optimize hot vapour filtration in a fast pyrolysis process.

References

Abatzoglou N, Gagnon M and Chornet E. (2002). Cold and hot gas filtration using a novel mobile granular bed with an inner fluidised section. The Canadian Journal of Chemical Engineering, vol. 80, no.1, pp. 17-27.

Agblevor F A, Besler S and Evans R J. (1995). Inorganic compounds in biomass feedstocks: Their role in char formation and effect on the quality of fast pyrolysis oils. In: Proceedings, Biomass pyrolysis oil properties and combustion meeting, September 26–28, Estes Park, Colorado. Milne, T. A. (Ed.). NREL-CP-430-7215, National Renewable Energy Laboratory, pp. 77-89.

Alakangas E, Koponen K, Sokka L and Keränen J. (2015). Classification of used wood to biomass fuel or solid recycled fuel and cascading use in Finland. For Boost for Entire Bioenergy Business, 2-4 September 2015, Jyväskylä, Finland. Book of Proceeding Bioenergy, pp. 79-86.

Aroussi A, Simmons K and Pickering S J. (2001). Particulate deposition on candle filters. Fuel, vol. 80, no. 3, pp. 335-343.

ASTM D4430-00. (2015). Standard practice for determining the operational comparability of meteorological measurements, ASTM International, West Conshohocken, PA, www.astm.org.

ASTM D5291-16. (2016). Standard test methods for instrumental determination of carbon, hydrogen, and nitrogen in petroleum products and lubricants, ASTM International, West Conshohocken, PA, www.astm.org.

ASTM D664-18e2. (2018). Standard test method for acid number of petroleum products by potentiometric titration, ASTM International, West Conshohocken, PA, www.astm.org.

ASTM D7544-12. (2017). Standard specification for pyrolysis liquid biofuel, ASTM International, West Conshohocken, PA, 2017, www.astm.org.

ASTM D7579-09. (2019). Standard test method for pyrolysis solids content in pyrolysis liquids by filtration of solids in methanol, ASTM International, West Conshohocken, PA, 2019, www.astm.org.

ASTM E203-16. (2016). Standard test method for water using volumetric Karl Fischer titration, ASTM International, West Conshohocken, PA, 2016, www.astm.org.

Ates F, Putun A E and Putun E. (2005). Fixed bed pyrolysis of Euphorbia rigida with different catalysts. Energy Conversion and Management, vol. 46, no. 3, pp. 421-432.

Autio J, Lehto J, Oasmaa A, Solantausta Y, Jokela P and Alin J. (2011). A pyrolysis pilot unit integrated to a circulating fluidised bed boiler - Experiences from a pilot project. 10th International Conference on Circulating Fluidized Beds and Fluidization Technology - CFB-10, T. Knowlton, PSRI Eds, ECI Symposium Series. https://dc.engconfintl.org/cfb10/19/.

Bahng M-K, Mukarakate C, Robichaud D J and Nimlos M R. (2009). Current technologies for analysis of biomass thermochemical processing: A review. Analytica Chimica Acta, vol. 651, no. 2, pp. 117-138.

Balat M, Balat M, Kırtay E and Balat H. (2009). Main routes for the thermo-conversion of biomass into fuels and chemicals. Part 1: Pyrolysis systems. Energy Conversion and Management, vol. 50, no. 12, pp. 3147-3157.

Baldwin R M and Feik C J. (2013). Bio-oil stabilization and upgrading by hot gas filtration. Energy Fuels, vol. 27, no. 6, pp. 3224-3238.

Biswas A K, Yang W and Blasiak W. (2011). Steam pretreatment of Salix to upgrade biomass fuel for wood pellet production. Fuel Processing Technology, vol. 92, no. 9, pp. 1711-1717.

Bridgwater A.V. and Peacocke G.V.C. (2000). Fast pyrolysis processes for biomass. Renewable and Sustainable Energy Reviews, vol. 4, no. 1, pp. 1-73.

Bridgwater AV. (2012). Review of fast pyrolysis of biomass and product upgrading. Biomass Bioenergy, vol. 38, pp. 68-94.

Bridgwater T. (2018). Challenges and opportunities in fast pyrolysis of biomass: Part 1. Johnson Matthey Technology Review, vol. 62, no. 1, pp. 118-130.

Brown R C, Shi H W, Colver G and Soo S C. (2003). Similitude study of a moving bed granular filter. Powder Technology, vol. 138, no. 2, pp. 201-210.

CEN – EN 16900. (2017). Fast pyrolysis bio-oils for industrial boilers – requirements and test methods, https://standards.globalspec.com/std/10201161/EN%2016900 (visited 2.4.2019).

CEN – TR 17103. (2017). Petroleum and related products - Fast pyrolysis bio-oils for stationary internal combustion engines - Quality determination, https://standards.globalspec.com/standards/detail?docId=10253238 (visited 2.4.2019).

Chen Y S and Hsiau S S. (2009). Cake formation and growth in cake filtration. Powder Technology, vol. 192, no. 2, pp. 217-224.

Chen Y S, Hsiau S S, Lai S C, Chyou Y P, Li H Y and Hsua C J. (2009). Filtration of dust particulates with a moving granular bed filter. Journal of Hazardous Materials, vol. 171, no. 1-3, pp. 987-994.

Chen T, Wu C, Liu R, Fei W and Liu S. (2011). Effect of hot vapour filtration on the characterization of bio-oil from rice husks with fast pyrolysis in a fluidized-bed reactor. Bioresource Technology, vol. 102, no. 10, pp. 6178-6185.

Chen Y S, Hsiau S S, Lee H Y and Chyou Y P. (2012). Filtration of dust particulates using a new filter system with louvers and sublouvers. Fuel, vol. 99, pp. 118-128.

Cummer K R and Brown R C. (2002). Ancillary equipment for biomass gasification. Biomass and Bioenergy, vol. 23, no. 2, pp. 113-128.

Czernik S and Bridgwater A V. (2004). Overview of Applications of biomass fast pyrolysis oil. Energy & Fuels, vol. 18, no. 2, pp. 590-598.

Demirbas A and Arin G. (2002). An overview of Biomass pyrolysis. Energy Source, vol. 24, no. 5, pp. 471-82.

Diebold J and Scahill J. (1988). Biomass to gasoline (BTG): Upgrading pyrolysis vapors to aromatic gasoline with zeolite catalysis at atmospheric pressure. ACS Symposium Series, vol. 376, pp. 264-276.

Diebold J P, Czernik S, Scahill J W, Philips S D and Feik C J. (1995). Hot gas filtration to remove char from pyrolysis vapors produced in the vortex reactor at NREL. In Proceedings, Biomass Pyrolysis Oil Properties and Combustion Meeting, September 26-28, Estes Park, Colorado, Milne T.A.Ed. NREL-CP-430-7215, National Renewable Energy Laboratory, pp. 90-108.

Diebold J P, Scahill, Czernik S, Philips S D and Feik C J. (1996). Progress in the production of hot-gas filtered biocrude oil at NREL. Bridgewater A V and Hogan E N (eds.), CPL press, pp. 66-81.

Diebold, J.P. (2002). A review of the chemical and physical mechanisms of the storage stability of fast pyrolysis bio-oils. Bridgwater A V (ed.), Fast pyrolysis of biomass, a handbook, CPL Press, vol. 2, pp. 243-292.

DIN 51900-1. (2000). Determining the gross calorific value of solid and liquid fuels using the bomb calorimeter, and calculation of net calorific value - Part 1: General information.

DOE Bioenergy Technologies Office (BETO) 2015 Project Peer Review Upgrading of Biomass Fast Pyrolysis Oil (Bio-oil). Website: https://www.energy.gov/sites/prod/files/2015/04/f21/thermochemical_conversion_abdullah_231401.pdf (Accessed on 21.2.2019)

Elliott D C and Baker E G. (1989). Process for upgrading biomass pyrolyzates. U.S. Patent 4795841.

Elliott D C, Wang H, French R, Deutch S and Lisa K. (2014). Hydrocarbon liquid production from biomass via hot-vapor-filtered fast pyrolysis catalytic hydroprocessing of the bio-oil. Energy Fuels, vol. 28, no. 9, pp. 5909-5917.

Garcia-Nunez J A, Palaez-Samaniego M R, Garcia-Perez M E, Fonts I, Abrego J, Westerhof R J M and Garcia-Perez M. (2017). Historical Developments of Pyrolysis Reactors: A Review. Energy Fuels, vol. 31, no. 6, pp. 5751-5775.

Heidenreich S. (2013). Hot gas filtration – A review. Fuel, vol. 104, pp. 83-94.

Hoekstra E, Hogendoorn K J A, Wang X, Westerhof R J M, Kresten S R A, van Swaaij W P M and Groeneveld M J. (2009). Fast pyrolysis of biomass in a fluidised bed reactor: In situ filtering of the vapors. Ind. Eng. Chem. Res., vol. 48, no. 10, pp. 4744-4756.

Hsiau S S, Smid J, Tsai F H, Kuo J T and Chou C S. (2004). Placement of flow-corrective elements in a moving granular bed with louvered-walls, Chemical engineering and processing, vol. 43, no. 8, pp. 1037-1045.

Javaid A, Ryan T, Berg G, Pan X, Vispute T, Bhatia S R, Huber G W and Ford D M. (2010). Removal of char particles from fast pyrolysis bio-oil by microfiltration. Journal of Membrane Science, vol. 363, no. 1-2, pp. 120-127.

Jones D D and Kocher M F. (1995). Auger design for uniform unloading of granular material: I. rectangular cross-section containers. American Society of Agricultural Engineers 38, no. 4, pp. 1157-1162.

Jung C H, Xiang R B, Kim M C, Lim K S and Lee K W. (2004). Performance evaluation of a cyclone with granular packed beds. Aerosol Science, vol. 35, no. 12, pp. 1483-1496.

Kan T, Strezov V and Evans T. J. (2016). Lignocellulosic biomass pyrolysis: A review of product properties and effects of pyrolysis parameters; Renewable and Sustainable Energy Reviews, volume 57, pp. 1126-1140.

Lehto J, Oasmaa A, Solantausta Y, Kytö M and Chiaramonti D. (2013). Fuel oil quality and combustion of fast pyrolysis bio-oils. VTT Technology, vol. 87. 79 p.

Liao H, Lu Q, Zhang Z and Dong C. (2013). Overview of methods to remove solid particles from biomass fast pyrolysis oils. Advanced Materials Research, vols. 608-609, pp. 265-268.

Liu Q, Chmely S C and Abdoulmoumine N. (2017). Biomass treatment strategies for thermochemical conversion. Energy Fuels, vol. 31, no. 4, pp. 3525-3536.

Liu Q, Labbé N, Adhikari S, Chmely S C. (2018). Hot water extraction as a pretreatment for reducing syngas inorganics impurities – A parametric investigation on switchgrass and loblolly pine bark. Fuel, vol. 220, pp. 177-184.

Mei Y, Liu R, Wu W and Zhang L. (2016). Effect of hot vapor filter temperature on mass yield, energy balance, and properties of products of the fast pyrolysis of pine sawdust. Energy Fuels, vol. 30, no. 12, pp. 10458-10469.

Meier D, Van de Beld B, Bridgwater A V, Elliott D C, Oasmaa A and Preto F. (2013). State-of-the-art of fast pyrolysis in IEA bioenergy member countries. Renewable and Sustainable Energy Reviews, vol. 20, pp. 619-641.

Mortensen P M, Grunwaldt J D, Jensen P A, Knudsen K G and Jensen A D. (2011). A review of catalytic upgrading of bio-oil to engine fuels. Applied Catalysis A: General, vol. 407, no. 1-2, pp. 1-19.

Oasmaa A, Kuoppala E and Solantausta Y. (2003). Fast pyrolysis of forestry residue. 2. Physicochemical composition of product liquid, Energy & Fuels, vol. 17, no. 2, pp. 433-443.

Oasmaa A, Peacocke C, Gust S, Meier D and McLellan R. (2005). Norms and standards for pyrolysis bio-oils. End-User Requirements and Specifications. Energy & Fuels, vol. 19, no. 5, pp. 2155-2163.

Oasmaa A, Elliott D C and Korhonen J. (2010). Acidity of biomass fast pyrolysis bio-oils. Energy fuels, vol. 24, no. 12, pp. 6548-6554.

Oasmaa A, Korhonen J and Kuoppala E. (2011). An approach for stability measurement of wood-based fast pyrolysis bio-oils. Energy Fuels, vol. 25, no. 7, pp. 3307-3313.

Oasmaa A, Sundqvist T, Kuoppla E, Garcia-Perez M, Solantausta Y, Lindfors C and Paasikallio V. (2015 a). Controlling the phase stability of biomass fast pyrolysis bio-oils. Energy Fuels, vol. 29, no. 7, pp. 4373-4381.

Oasmaa A, Beld B V D, Saari P, Elliott D C and Solantausta Y. (2015 b). Norms, Standards, and legislation for Fast Pyrolysis Bio-oils from Lignocellulosic Biomass. Energy Fuels, vol. 29, no. 4, pp. 2471-2484.

Paasikallio V. (2016). Bio-oil production via catalytic fast pyrolysis of woody biomass. Aalto University publication series, Doctoral Dissertations 227, VTT Science 137, pp. 95 + app. 71.

Paenpong C, Pattiya A. (2016). Effect of pyrolysis and moving-bed granular filter temperatures on the yield and properties of bio-oil from fast pyrolysis of biomass. Journal of Analytical and Applied Pyrolysis, vol. 119, pp. 40-51.

Pan W-P and Richard G N. (1989). Influence of metal ions on volatile products of pyrolysis of wood. Journal of Analytical and Applied Pyrolysis, vol. 16, no. 2, pp. 117-126.

Pattiya A and Suttibak S. (2012 a). Production of bio-oil via fast pyrolysis of agricultural residues from cassava plantations in a fluidised-bed reactor with a hot vapour filtration unit. Journal of Analytical and Applied Pyrolysis, vol. 95, pp. 227-235.

Pattiya A and Suttibak S. (2012 b). Influence of a glass wool hot vapour filter on yields and properties of bio-oil derived from rapid pyrolysis of paddy residues. Bioresource Technology, vol. 116, pp. 107-113.

Perkins G, Bhaskar T, Konarova M. (2018). Process development status of fast pyrolysis technologies for the manufacture of renewable transport fuels from biomass. Renewable and Sustainable Energy Reviews, vol. 90, pp. 292-315.

Powell J B. (2010) Sustainable innovation in the chemical industry and its commercial impacts, in Harmsen J and Powell J B (eds.) (2010). Sustainable development in the process industries: case and impact. John Wiley & Sons, pp. 209-216.

Rubow K L, Huang B, Wilson M and Mahon E. (2006). Hot gas filtration using sintered metal filters. Mott Corporation, 4th China international conference.

San Miguel G, Makibar J and Fernandez-Akarregi A R. (2012). New Advances in the Fast Pyrolysis of Biomass. Biobased Materials and Bioenergy, vol. 6, no. 2, pp. 1-11.

Scahill J, Diebold J P and Feik C. (1997). Removal of Residual Char Fines from Pyrolysis Vapors by Hot Gas Filtration. In: Bridgwater A V and Boocock D G B. (eds.) Developments in Thermochemical Biomass Conversion. Springer, Dordrecht, pp. 253-266.

SFS-EN ISO 16948. (2015). Solid biofuels, determination of total content of carbon, hydrogen and nitrogen. Finnish standard association.

SFS-EN ISO 18122. (2015). Solid biofuels, determination of ash content. Finnish standard association.

SFS-EN ISO 18123. (2015). Solid biofuels, determination of the content of volatile matter. Finnish standard association.

SFS-EN ISO 18125. (2017). Solid biofuels, determination of calorific value. Finnish standard association.

SFS-EN ISO 18134-3. (2015). Solid biofuels. Determination of moisture content. Oven dry method. Part 3: Moisture in general analysis sample. Finnish standard association.

Sharifzadeh M, Sadeqzadeh M, Guo M, Borhani T N, Murthy Konda N V S N, Garcia M C, Wang L, Hallett J and Shah N. (2019). The multi-scale challenges of biomass fast pyrolysis and bio-oil upgrading: Review of the state of art and future research directions. Progress in Energy and Combustion Science, vol. 71, pp. 1-80.

Si Z, Zhang X, Wang C, Ma L and Dong R. (2017). An overview on catalytic hydrodeoxygenation of pyrolysis oil and its model compounds. Catalysts, vol. 7, no. 6, 169 p.

Sitzmann J. (2009). Upgrading of Fast Pyrolysis Oils by Hot Filtration. Doctor of Philosophy Dissertation, Aston University.

Solantausta Y, Gust S, Hogan E, Massoli E and Sipilä K. (2001). Bio-oil fuel oil - Upgrading by hot filtration and novel physical methods. VTT Technical Research of Finland, 49 p.

Stefanidis S D, Heracleous E, Patiaka D T, Kalogiannis K G, Michailof C M and Lappas A A. (2015). Optimization of bio-oil yields by demineralization of low quality biomass. Biomass and Bioenergy, vol. 83, pp. 105-115.

Sundqvist T, Oasmaa A and Koskinen A. (2015). Upgrading fast pyrolysis bio-oil quality by esterification and azeotropic water removal. Energy Fuels, vol. 29, pp. 2527-2534.

Venderbosch R H and Prins W. (2010). Fast pyrolysis technology development. Biofuels, Bioproducts Biorefining, vol. 4, no. 2, pp. 178-208.

Wang H, Elliott D C, French R J, Deutch S and Lisa K. (2016). Biomass conversion to produce hydrocarbon liquid fuel via hot-vapor filtered fast pyrolysis and catalytic hydrotreating. Journal of Visualized Experiments, vol. 118, e54088, 13 p.

Xiao G, Wang X, Zhang J, Ni M, Gao X, Luo Z and Cen K. (2013). Granular bed filter: A promising technology for hot gas clean-up. Powder Technology, vol. 244, pp. 93-99.

APPENDIX 1. Dry mass balance (132, 133 and 134)

Parameters	Unit	Run		
Run		132	133	134
Pyrolysis temperature	°C	500	480	520
Run time	h	3	3	3
Inputs				
Amounts of raw materials	g	2175	2446	2173
Raw material feed (wet)	g/h	725	815	724
Raw material moisture content	wt. %	7.7	7.2	6.9
Raw material feed (dry)	g/h	669	757	675
Total amount of nitrogen	nl/min	34	34	34
Outputs				
Cyclone chars	g	298	349	299
Organic liquid (ESP + condensers)	g	1099	1237	1045
Pyrolytic water	g	216	267	228
Total water	g	382	442	377
Pyrolytic gases	g	258	273	321
Mass balance (dry)				
Cyclone chars	wt. %	15	15	15
Pyrolytic gases	wt. %	13	12	16
Organic pyrolytic liquid	wt. %	55	54	52
Pyrolytic water	wt. %	11	12	11
Amount of products	wt. %	93	94	94
Bio-oil yield	wt. %	65	66	63

APPENDIX 2. Dry mass balance (135, 136 and 137)

Parameters	Unit	Run		
Run		135	136	137
Filtration temperature	°C	450	400	360
Run time	h	6	6	6
Face velocity	cm/s	1.1-1.2		
Inputs				
Amounts of raw materials	g	3568	3721	4281
Raw material feed (wet)	g/h	595	620	714
Raw material moisture content	wt.%	7.8	8.1	7.4
Raw material feed (dry)	g/h	548	570	661
Total amount of nitrogen	nl/min	36	36	36
Outputs				
Cyclone chars	g	488	475	612
Filter chars	g	89.5	95.0	84
Organic liquid (ESP + condensers)	g	1320	1593	1913
Pyrolytic water	g	345	370	425
Total water	g	623	671	740
Pyrolytic gases	g	564	502	513
Mass balance (dry)				
Cyclone chars	wt. %	15	14	15
Filter chars	wt. %	3	3	2
Pyrolytic gases	wt. %	17	15	13
Organic pyrolytic liquid	wt. %	40	47	48
Pyrolytic water	wt. %	10	11	11
Amount of products	wt. %	85	89	89
Bio-oil yield	wt. %	51	57	59
Total char yield	wt. %	18	17	18

APPENDIX 3. Pilot-scale preliminary calculations

Pilot-scale input parameters				
Parameters	Unit	Calculations		
Candle diameter	cm	6		
Length of the filter vessel	cm	101		
Length of the filter vessel without wall thickness	cm	100		
Width of the filter vessel	cm	44		
layout area of filter vessel	m2	0.44		
Filter candles area (9 candles)	m2	1.70		
Design face velocity	cm/s	2.03		
Moisture content of raw material	wt. %	10		
Raw material feed	kg/h	20		
Utilized fluidization velocities	m/s	4	5	8
Fluidization gas	nl/min	281	351	561
Water	l/min	86	86	86
Organics	l/min	23	23	23
Gases	l/min	63	63	63
Sum of products	l/min	453	528	733
Pilot-scale face velocity calculation				
Gases (T=500 °C)	l/min	1282	1495	2077
Minimum required surface area for the design face velocity	m2	1.05	1.23	1.71
Face velocity of 9 candles filter vessel	cm/s	1.26	1.47	2.04

Used calculations:

$$Filter\ candles\ area\ (9\ candles) = 2 * \pi * r * l$$

$$Gases\ (T = 500\ ℃) = \frac{(273.15 + 500) * Sum\ of\ products}{273.15}$$

$$Minimum\ required\ surface\ area\ for\ the\ design\ face\ velocity = \frac{Gases\ (T = 500\ ℃)}{Design\ face\ velocity}$$

$$Face\ velocity\ of\ 9\ candles\ filter\ vessel = \frac{Gases\ (T = 500\ ℃)}{Filter\ candles\ area\ (9\ candles)}$$

APPENDIX 4. Pilot-scale dimensions calculations (1/3)

Parameters	Unit	Values	
Vessel length	cm	101	
Filter candle length	cm	100	
Section 1 dimensions		With wall thickness	Without wall thickness
Height	cm	19.75	19.75
Width	cm	44	43
Diameter of sand tubes	cm	12.5	11.5
Volume 1	L	25.05	24.81
Sand inlet tubes volume	L	1.23	1.04
Volume 2	L	87.77	84.93
Total volume	L	61.49	59.08
Section 2 dimensions			
Height	cm	12	12
Width	cm	44	43
Total volume	L	53.3	51.6
Candles volume	L	11.42	
Sand volume	L	40.18	
Section 3 dimensions			
Height	cm	10	10
Width	cm	44	43
Total volume	L	44.44	43
Candles volume	L	11.42	
Sand volume	L	31.58	
Section 4 dimensions			
Height	cm	14.5	14.5
Top width	cm	44	43
Bottom width	cm	15	
Volume 3	L	64.44	62.35
Volume 4	L	21.24	21.03
Total volume	L	43.20	41.33
Candle volume	L	2.86	
Sand volume	L	38.47	

APPENDIX 4. Pilot-scale dimensions calculations (2/3)

Filter capacity and dimensions		With wall thickness	Without wall thickness
Total volume of the vessel	L	202.5	195.01
Sand volume in filter [Required min]	L	110.2	
Total candles volume	L	25.7	
Cased Auger screw diameter	cm	30	
Filter vessel height	cm	86.25	
Filter vessel width	cm	44	
Filter vessel length	cm	101	
Carbon Steel density	kg/m^3	7850	
Carbon Steel volume in vessel with 5 mm wall thickness	m^3	0.01	
Vessel weight	kg	58.51	

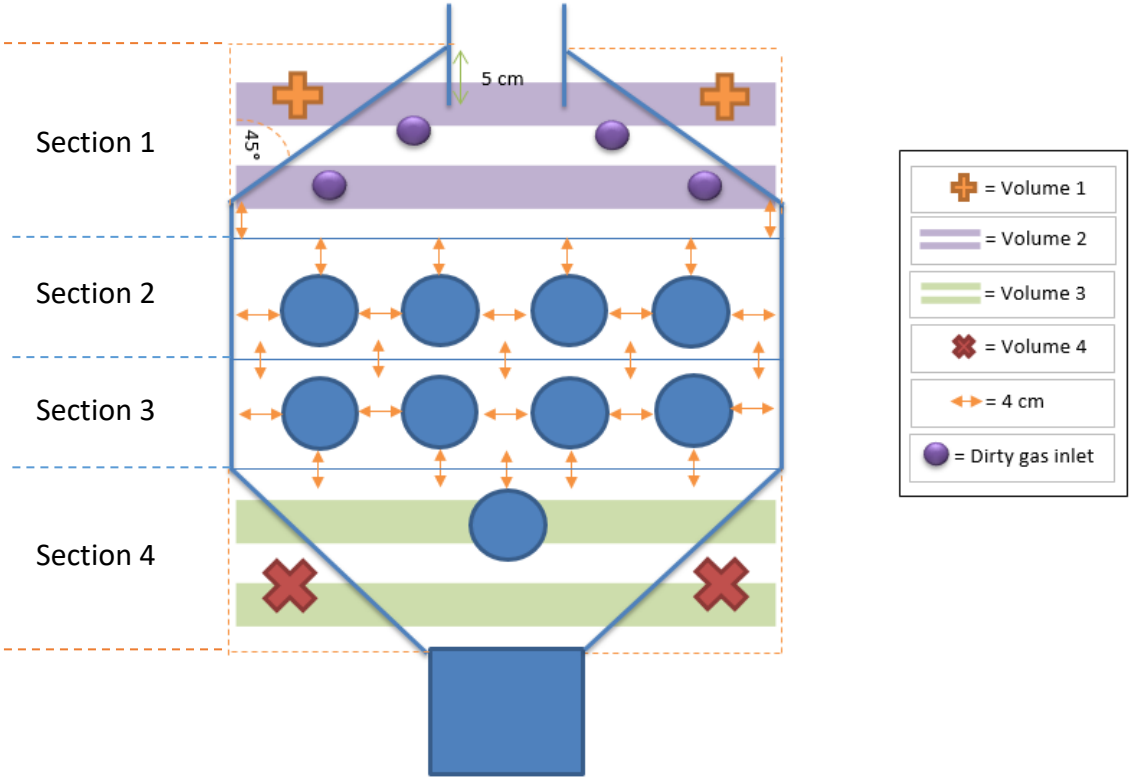

APPENDIX 4. Pilot scale dimensions calculations (3/3)

Used calculations:

$$Volume\ (section\ 1) = Volume\ 2 - Volume\ 1 - Sand\ inlet\ tubes\ volume$$

$$Volume\ (section\ 2) = Height * Width * Length$$

$$Volume\ (section\ 3) = Height * Width * Length$$

$$Volume\ (sand) = Volume\ of\ section\ X\ (without\ thickness) - Volume\ of\ candles$$

$$Volume\ (section\ 4) = Volume\ 3 - Volume\ 4$$

$$Total\ volume\ of\ vessel = Volume\ (section\ 1) + Volume\ (section\ 2) + Volume\ (section\ 3) + Volume\ (section\ 4)$$

Carbon steel volume with 5 mm wall thickness

$$= Total\ volume\ (with\ wall\ thick.) - Total\ volume\ (without\ wall\ thick.)$$

$$Vessel\ weight = Volume\ (Carbon\ steel) * Density\ (Carbon\ steel)$$

APPENDIX 5. Pilot-scale sand calculations (1/2)

Inputs		
Parameters	Unit	Values
Filter vessel length	cm	100
Bottom width (conveyor)	cm	15
Sand volume in pilot-scale filter [Required min]	L	110.22
Sand volume in bench scale filter [Required min]	L	11.802
Max. Sand flow in bench scale filter	l/h	2.076
Min. Sand flow in bench scale filter	l/h	1.04
Sand flux calculations		
Max. sand flow (Pilot-scale)	l/h	19.39
Min. sand flow (Pilot-scale)	l/h	9.69
Sand change at max. sand flow	h	5.68
Sand change at min. sand flow	h	11.37
Surface area in-between top candles	m2	0.2
Max. sand flow	m3/s	5.39E-06
Max. sand volumetric flux	cm/s	0.0027
Min. sand flow	m3/s	2.69E-06
Min. sand volumetric flux	cm/s	0.0013
Surface area across bottom conveyor	m2	0.15
Max. sand volumetric flux	cm/s	0.0036
Min. sand volumetric flux	cm/s	0.0018

Used calculations:

$$Max.\,sand\ flow\ (Pilot\ scale) = Sand\ volume\ (Pilot\ scale) * \left(\frac{Max.\,sand\ flow\ (Bench\ scale)}{Sand\ volume\ (Bench\ scale)}\right)$$

$$Min.\,sand\ flow\ (Pilot\ scale) = Sand\ volume\ (Pilot\ scale) * \left(\frac{Min.\,sand\ flow\ (Bench\ scale)}{Sand\ volume\ (Bench\ scale)}\right)$$

$$Sand\ change\ at\ max.\,sand\ flow = \frac{Sand\ volume}{Max.\,sand\ flow}$$

$$Sand\ change\ at\ min.\,sand\ flow = \frac{Sand\ volume}{Min.\,sand\ flow}$$

$$Surface\ area\ between\ top\ candles = 5 * 4\ cm\ (space) * Vessel\ length$$

$$Max.\,sand\ volumetric\ flux = \frac{Max.\,sand\ flow}{Surface\ area\ between\ top\ candles}$$

APPENDIX 5. Pilot-scale sand calculations (2/2)

$$Min.volumetric\ flux = \frac{Min.sand\ flow}{Surface\ area\ between\ top\ candles}$$

$$Surface\ area\ across\ bottom\ conveyor = Vessel\ length * Bottom\ width\ (conveyor)$$

$$Max.sand\ volumetric\ flux = \frac{Max.sand\ flow}{Surface\ area\ across\ bottom\ conveyor}$$

$$Min.volumetric\ flux = \frac{Min.sand\ flow}{Surface\ area\ across\ bottom\ conveyor}$$